

CANINE GAIT ANALYSIS AND DIAGNOSIS  
USING ARTIFICIAL NEURAL NETWORKS  
AND  
GROUND REACTION FORCE

by

MAKIKO KAIJIMA

(Under the direction of Ronald W. McClendon)

ABSTRACT

Artificial neural networks (ANNs) were developed to map ground reaction force (GRF) data to subjective diagnostic scores of lameness. Twenty-one clinically normal dogs (19–32.2 kg) underwent surgery inducing osteoarthritis in the left hind stifle joint. Lameness scores were assigned by a veterinarian and GRF data were collected twice prior to and five times after the surgery. The study discussed herein focused on identifying the preferred ANN architecture and input variables extracted from GRF curves. The data were partitioned to allow the accuracy of the resulting models to be evaluated with dogs not included in model development. The results indicate that backpropagation neural networks are preferable to probabilistic neural networks. Input variables were identified in this study that capture a dog's attempt to remove weight from an injured limb. ANNs differentiated the three classes of lameness with an accuracy ranging from 87.8–100%.

INDEX WORDS: Canine, Dog, Gait Analysis, Artificial Neural Network, Ground Reaction Force, Diagnosis, Biomechanics, Force Plate, Lameness, Probabilistic Neural Network, Backpropagation, Decision Support

CANINE GAIT ANALYSIS AND DIAGNOSIS  
USING ARTIFICIAL NEURAL NETWORKS  
AND  
GROUND REACTION FORCE

by

MAKIKO KAIJIMA

B.A., Keio University, Japan 2000

A Thesis Submitted to the Graduate Faculty  
of The University of Georgia in Partial Fulfillment  
of the  
Requirements for the Degree

MASTER OF SCIENCE

ATHENS, GEORGIA

2005

© 2005

Makiko Kaijima

All Rights Reserved

CANINE GAIT ANALYSIS AND DIAGNOSIS  
USING ARTIFICIAL NEURAL NETWORKS  
AND  
GROUND REACTION FORCE

by

MAKIKO KAIJIMA

Approved:

Major Professor: Ronald W. McClendon

Committee: Timothy L. Foutz  
Walter D. Potter

Electronic Version Approved:

Maureen Grasso  
Dean of the Graduate School  
The University of Georgia  
May 2005

## DEDICATION

For my family

I would like to dedicate this thesis to my parents, Tadao and Kiyoko Kaijima, who tremendously encouraged and supported my education at home and abroad. I also would like to dedicate it to my sister, Sawako Kaijima, who has been a great inspiration throughout my life and motivated me to achieve higher goals.

## ACKNOWLEDGMENTS

I would like to thank all of the professors and friends for their support and guidance.

First of all, I would like to express my gratitude to all of my committee members. Especially, I would like to thank my major professor, Dr. Ron McClendon, for providing me with valuable knowledge about Artificial Neural Networks and introducing me to this project and its members. I also wish to thank Dr. Tim Foutz for sharing his insightful Biomechanics knowledge and guiding me through my thesis work. My great appreciation also goes to Dr. Don Potter for having equipped me with a set of skills versatile enough to solve a variety of problems throughout the Masters degree program.

I also would like to thank Dr. Steven Budsberg for letting me use the precious data he has collected over years and for sharing his Veterinary Medicine expertise. In addition, I would like to thank Lisa Reynolds for helping me become familiar with the data, data acquisition procedure, and other related materials. Furthermore, I would like to thank all of my friends, especially Shilpa Hardas, Jaymin Kessler, Soyoung Kwon, and Rabia Guendouzen for constantly providing intellectual stimulus and mental support. I would also like to thank Matthew Horton for helping me with my English and proofreading this thesis.

I also would like to thank Dr. Michael Covington for not only providing me with valuable AI and computer-related skills but also sharing his valuable study strategies for maintaining the highest academic standards.

Lastly, I would like to thank Dr. Don Nute for introducing me to this exciting field of AI.

My academic goals became quite different from the ones I had originally planned. I came here to make my longtime dream of becoming an athletic trainer come true. Taking many classes in different areas and meeting people with high academic standards, I decided to switch my major. I am grateful for all of your invaluable guidance and sage advice. Without

all of your synergistic support, I could not have excelled in a new field and completed my Masters degree. Once again, thank you very much; the technical and human skills I have obtained here will remain a lifelong treasure.

## TABLE OF CONTENTS

	Page
ACKNOWLEDGMENTS . . . . .	v
LIST OF FIGURES . . . . .	ix
LIST OF TABLES . . . . .	xi
CHAPTER	
1 INTRODUCTION . . . . .	1
1.1 PROBLEMS IN CANINE GAIT ANALYSIS . . . . .	1
1.2 ADVANTAGES AND EFFECTIVENESS OF FORCE-PLATE CANINE GAIT ANALYSIS . . . . .	2
1.3 CLASSIFICATION TECHNIQUES FOR GAIT ABNORMALITY DETECTION	3
1.4 DESCRIPTION OF THE STUDY . . . . .	5
2 FUNDAMENTALS OF CANINE GAIT . . . . .	7
2.1 TERMINOLOGY . . . . .	7
2.2 TYPES OF GAIT . . . . .	8
2.3 GRF CURVE . . . . .	9
3 METHODOLOGY . . . . .	18
3.1 DATA COLLECTION TOOLS AND PROCEDURE FOR THE PHARMA- CEUTICAL STUDY . . . . .	18
3.2 DATA SET PREPARATION . . . . .	19
3.3 ANN DESIGN TOOL AND PROCEDURE . . . . .	19
4 RESULTS AND DISCUSSION . . . . .	42

4.1	PRELIMINARY INPUT ANALYSIS AND IMPORTANT SINGLE INPUT VARIABLES . . . . .	42
4.2	SELECTION OF PREFERRED ANN MODEL AND SETS OF INPUT VARIABLES . . . . .	43
4.3	SELECTION OF PREFERRED NUMBER OF BPN HIDDEN NODES . .	46
4.4	PREFERRED ANN MODEL AND SET OF INPUT VARIABLES . . . .	47
5	SUMMARY AND CONCLUSIONS . . . . .	63
5.1	SUMMARY . . . . .	63
5.2	CONCLUSIONS . . . . .	64
	REFERENCES . . . . .	70

## LIST OF FIGURES

2.1	Footfall Sequence of Symmetrical Gait . . . . .	13
2.2	Rhythm of Footfalls in Symmetrical Gait . . . . .	13
2.3	Orthogonal Components of GRF . . . . .	13
2.4	Representative GRF Curves of Normal Canine Gait . . . . .	14
2.5	Representative Vertical GRF Curves of Normal and Abnormal Canine Gait .	15
2.6	Representative Cranial-Caudal GRF Curves of Normal and Abnormal Canine Gait . . . . .	16
2.7	Representative Medial-Lateral GRF Curves of Normal and Abnormal Canine Gait . . . . .	17
3.1	BPN with One Output Node to Differentiate Three Classes . . . . .	36
3.2	BPN with Three Output Nodes to Differentiate Three Classes . . . . .	36
3.3	PNN with Three Output Nodes to Differentiate Three Classes . . . . .	36
3.4	Vertical GRF Input Variables . . . . .	37
3.5	Cranial-Caudal GRF Input Variables . . . . .	38
3.6	Medial-Lateral GRF Input Variables . . . . .	39
3.7	Input Variables Related to Mid Point . . . . .	40
3.8	Shift in Center of Gravity during Abnormal Gait . . . . .	41
4.1	BPN with Three Output Nodes Using Mid(R-L)/FRONT, Mid(R-L)/HIND, and PFz(RH) (Data Configuration 1) . . . . .	58
4.2	PNN Using Mid(R-L)/FRONT, Mid(R-L)/HIND, and PFz(RH) (Data Con- figuration 1) . . . . .	59
4.3	BPN with One Output Node Using Mid(R-L)/FRONT, Mid(R-L)/HIND, PFz(RF), PFz(RH), AveF(RF), and AveR(RH) (Data Configuration 1) . . .	60

4.4	Hidden Node Analysis (BPN with One Output Node) . . . . .	61
4.5	Hidden Node Analysis (BPN with Three Output Nodes) . . . . .	62
5.1	LM1 and LM3 Vertical GRF Curves Acquired from Dog A . . . . .	69

## LIST OF TABLES

3.1	Subjective Scoring System . . . . .	27
3.2	Number of Patterns Acquired at Every Observation Point . . . . .	28
3.3	Score Obtained for Each Dog at Each Observation Point . . . . .	29
3.4	Number of Patterns Acquired for Each Dog . . . . .	30
3.5	ANN Architecture Parameters . . . . .	31
3.6	Input Variables Provided by the Software . . . . .	32
3.7	Input Variables Calculated from the Variables Listed in Table 3.6 . . . . .	32
3.8	Input Variables Calculated from the Raw Data . . . . .	33
3.9	Target Value Coding (BPN with One Output Node) . . . . .	34
3.10	Target Value Coding (BPN with Three Output Nodes) . . . . .	34
3.11	Target Value Coding (PNN with Three Output Nodes) . . . . .	34
3.12	Two Data Configurations . . . . .	35
3.13	Number of Patterns in Data Configurations 1 and 2 . . . . .	35
4.1	Overall Accuracy (%) Using a Conventional Single Input Variable, Data Configuration 1, Evaluation Data Set . . . . .	48
4.2	Overall Accuracy (%) Using a Single Input Variable Suggested in This Study, Data Configuration 1, Evaluation Data Set . . . . .	48
4.3	Overall Accuracy (%) Using Combinations of the Three Best Single Input Variables, Data Configuration 1, Evaluation Data Set . . . . .	49
4.4	Overall Accuracy (%) Using Mid(R-L)/FRONT, Mid(R-L)/HIND and Other Variables, Data Configuration 1, Evaluation Data Set . . . . .	50
4.5	Overall Accuracy (%) Using Mid(R-L)/FRONT, Mid(R-L)/HIND and Other Variables, Data Configurations 1 and 2, Evaluation Data Sets . . . . .	51

4.6	Misclassification by BPN with One Output Node, Data Configuration 1, Evaluation Data Set . . . . .	52
4.7	Misclassification by BPN with Three Output Nodes, Data Configuration 1, Evaluation Data Set . . . . .	53
4.8	Misclassification by PNN, Data Configuration 1, Evaluation Data Set . . . .	54
4.9	Misclassification by BPN with One Output Node, Data Configuration 2, Evaluation Data Set . . . . .	55
4.10	Misclassification by BPN with Three Output Nodes, Data Configuration 2, Evaluation Data Set . . . . .	56
4.11	Misclassification by PNN, Data Configuration 2, Evaluation Data Set . . . .	57

## CHAPTER 1

### INTRODUCTION

#### 1.1 PROBLEMS IN CANINE GAIT ANALYSIS

##### 1.1.1 HISTORY AND CURRENT STATE OF GAIT ANALYSIS

Scientific studies on canine locomotion started in the late nineteenth century (Brown, 1986; DeCamp, 1997; Hollenbeck, 1981; Newton & Nunamaker, 1985). Subsequently, various gait analysis methods have been proposed, such as kinetic analysis of ground reaction force (GRF) obtained from force-plates, computer-aided 3-D kinematic analysis of the motor relationship between each body segment, and assessment of electromyography (EMG)<sup>1</sup> and electrogoniometry (EGM)<sup>2</sup> (DeCamp, 1997; Newton & Nunamaker, 1985). In the last twenty years, these techniques have been increasingly used in clinical practice along with subjective diagnoses. Force-plate and kinematic analysis are widely accepted and have been proven to be a reliable means of assessing normal and abnormal gait and the efficacy of various medical interventions (Budberg, 2001; Budberg et al., 1987, 1988, 1993, 1995, 1996, 1999; Cross et al., 1997; DeCamp, 1997; Dueland et al., 1977, Jevens et al., 1996; McLaughlin, 2001; O'Connor et al., 1989; Renberg et al., 1999).

##### 1.1.2 PROBLEM STATEMENT

The accuracy and consistency of subjective gait evaluations are limited by a clinician's knowledge, experience, and observational acumen. Force-plate and kinematic analyses provide objective, quantifiable, and repeatable results of canine gait evaluation by eliminating

---

<sup>1</sup>EMG measures the electrical activity of muscles.

<sup>2</sup>EGM is a technique used to gather information about the angles of the joint.

human bias (McLaughlin, 2001). These analyses also accelerate data collection procedures. However, data obtained using these methods are not fully exploited in current veterinary practice. Researchers are often baffled by the massive quantities of data obtained from these measurement tools. Moreover, data recorded from signal devices make it difficult to extract important clinical information. The relationships between subjective diagnostic scores given by veterinarians and objective GRF data are not yet fully understood, even though correlations have been found between them (Budberg et al., 1988, 1996; Jevens et al., 1996). However, the results of objective gait analysis must correspond with clinical assessment of diseases and their treatment. Although force-plate analysis is not an alternative to subjective diagnosis, gait analysis can be used to enhance diagnostic accuracy. As a result, there is a need for an automated process that fully exploits the available data, performs biomechanical analysis on them, and relates the results to subjective evaluation for an accurate, reliable, and efficient clinical decision making procedure.

## 1.2 ADVANTAGES AND EFFECTIVENESS OF FORCE-PLATE CANINE GAIT ANALYSIS

The advantage of force-plate analysis is that it readily acquires reliable GRF data for assessing the limb function of a dog. A gait involves a complicated musculoskeletal coordination mechanism. For example, a limb must apply a vertical force against the hip or shoulder to support its weight and must apply a forward force along the vertebral column to move forward. In addition, according to Newton's First Law, a dog must elicit a force from its external environment to move or change its speed or direction. In other words, a dog needs to push off the ground and simultaneously receive environmental resistance. This resistance force is then applied back to the limb and transmitted to the whole system, which causes the motion of the next limb. This iterative process results in a gait (Gray, 1968).

A thorough functional analysis of a canine gait requires detailed knowledge of a large amount of biological information: changes in tension and length of individual muscles and the anatomical relationships between different muscles and between muscle and bone. Measuring

these changes and relationships accurately without interfering with a dog’s movement is difficult and impractical. However, if we regard the body as a single musculoskeletal functional unit, we can assess the combined effort of all the parts of the system involved in locomotion by letting the dog walk on force-plates. According to Newton’s Third Law, orthogonal reaction forces are exactly equal in magnitude but opposite in direction to the net internal force generated by the whole system, which is transmitted through a limb to the ground (Gray, 1968). Hence, even though GRF tests cannot measure joint-specific or muscle-specific functions during locomotion, they can measure limb functions to a great extent. Thus, the results of tests performed on force-plates are important. For a more detailed description of canine gait biomechanics, see Brown (1986), Gray (1968), and Hollenbeck (1981).

### 1.3 CLASSIFICATION TECHNIQUES FOR GAIT ABNORMALITY DETECTION

Several classification techniques have been applied to gait data for differentiating normal and abnormal gait, such as mathematical and statistical methods, fractal dynamics, wavelet transformation, and artificial intelligence techniques such as machine learning, fuzzy clustering, and artificial neural networks (ANNs) (Barton & Lees, 1997; Begg & Kamruzzaman, 2005; Chau, 2001 [a] & [b]; Cheron et al., 2003; Evans et al., 2003; Hahn et al., 2005; Keegan et al., 2003; Lafuente et al., 1997; O’Malley et al., 1997; Schobesberger & Peham, 2002; Schöllhorn, 2004; Simon, 2004; Su & Wu, 2000; Wu et al., 2001).

Evans et al. (2003) applied a decision rule called Youden’s index to GRF data obtained from a total of 76 Labrador retrievers, 69 of which had unilateral cranial cruciate disease. They differentiated normal and abnormal gait with 78.3–82.6% sensitivity<sup>3</sup> and 82.3–88.2% specificity<sup>4</sup> using peak vertical forces and impulses.

Recently, ANNs have been used for human gait analysis (Chau, 2001[b]) and have also been used for equine gait analysis (Keegan et al., 2003; Schobesberger & Peham, 2002). ANNs

---

<sup>3</sup>The frequency of classifying a normal dog as normal

<sup>4</sup>The frequency of classifying an abnormal dog as abnormal

have been used to process several types of gait data, including GRFs, foot pressure, joint angles, and EMGs (Chau, 2001[b]). An ANN is a computational model that simulates the biological learning process of a brain. There are many types of ANNs, but all consist of three elements: processing units called nodes, links connecting each of them, and mathematical learning rules. In supervised learning, an ANN learns by example rather than by using domain-specific knowledge. In supervised training, the ANN goes through a large number of examples of a known set of inputs and corresponding outputs. For example, Backpropagation Networks (BPNs) determine the relationships between the inputs and outputs by adjusting weights associated with each link through an iterative procedure.

Keegan et al. (2003) used ANNs to process kinematic data that were obtained from horses trotting on a treadmill and transformed using the continuous wavelet transformation method. The ANN model differentiated three classes of lameness (i.e., normal and lameness in the left or right front limb) with an accuracy of 85%. Schobesberger and Peham (2002) used ANNs to process kinematic data that were obtained from horses trotting on a treadmill and transformed by the Fast-Fourier-Transformation algorithm. Their ANN model differentiated six classes of lameness with an accuracy of 78%.

Su and Wu (2000) and Wu et al. (2001) used ANNs to map GRF data obtained from healthy human subjects and patients with ankle arthrodesis. A total of 18 input variables extracted from GRF curves were used. Half of the input variables were force parameters normalized by mass: the peak vertical forces at (1) heel-strike and (2) push-off, (3) the minimum vertical force at mid stance, (4) the peak fore-aft forces at heel-strike, the peak (5) braking and (6) propulsive forces, and the peak medial-lateral forces at (7) heel strike, (8) mid-stance, and (9) push-off. The rest of the input variables were temporal variables corresponding to each force parameter normalized by the duration of the stance phase. Using all 18 input variables, the standard 3-layer BPN differentiated normal and abnormal gait 89% accurately. Better results of 98% were obtained using a Genetic Algorithm Neural Network (GANN), which used a genetic algorithm to find the optimal set of input variables.

The input variables found to be useful for GANN included force parameters (1) and (4)–(8) and temporal parameters (2), (4) and (8). For more studies that used ANNs to process gait data, see Barton & Lees (1997), Chau (2001 [b]), Cheron (2003), Hahn et al. (2005), Lafuente et al. (1997), Schöllhorn (2004), and Simon (2004).

One of the major advantages of using ANNs to process gait data for diagnostic problems is that they can be developed without full knowledge of the domain. Since they are data-driven, one need not be certain how each factor in the data interact or contribute to the final results. Therefore, ANNs can be used for a clinical decision support system, which must account for how noisy, ambiguous, or distorted medical data might be associated with a particular symptom. In addition, ANNs can generalize well on a new set of data. In other words, ANNs can use previously known information to draw conclusions about similar but not identical observation. This characteristic of ANNs is especially valuable because a new patient is unlikely to have exactly the same medical condition as previously seen patients. However, these systems are black-box in nature and cannot provide explanations for the results. In addition, it has been shown that the accuracy of ANN output improves with higher numbers of observations (Smith, 1993). Since the number of medical observations could be scarce, and the network could become more susceptible to the noise in data.

## 1.4 DESCRIPTION OF THE STUDY

### 1.4.1 PURPOSE AND SIGNIFICANCE OF THE STUDY

GRF reflects a dog's movement and its inside musculoskeletal activity as a whole. ANNs are well suited for classification using noisy biomedical data from a signal device, and they have been shown to be an effective means for detecting human and equine gait abnormalities (Barton & Lees, 1997; Chau, 2001 [b]; Cheron et al., 2003; Hahn et al., 2005; Keegan et al., 2003; Lafuente et al., 1997; O'Malley et al., 1997; Schobesberger & Peham, 2002; Schöllhorn, 2004; Simon, 2004; Su & Wu, 2000; Wu et al., 2001). Therefore, an ANN could be trained using canine GRF data to accurately predict the subjective diagnosis of a veterinarian.

If successfully implemented in a decision support system, ANNs developed for canine gait analysis and diagnosis could have a significant clinical impact. More accurate diagnosis supported by computerized analysis of objective GRF data could result in the detection of subtle lameness, which is often missed by a clinician. In addition, it could enable much more precise evaluation of surgical and pharmacological intervention. Moreover, ANNs can be used for educational purposes.

#### 1.4.2 GOAL AND OBJECTIVES

The goal of this study was to determine the accuracy of ANNs used to map variables extracted from GRF curves to a subjective diagnostic score of lameness.

The related objectives of this study were to

1. identify the input variables extracted from GRF curves that could be used to duplicate accurately the subjective diagnostic score of lameness,
2. find the preferred ANN architecture and combinations of input variables, and
3. to evaluate the feasibility and accuracy of the results for use in an automated canine lameness diagnostic system.

#### 1.4.3 ORGANIZATION OF THE STUDY

Chapter 2 summarizes important terminology related to canine gait and the interpretation of GRF curves. The clinical data and ANNs used in this study are explained in Chapter 3. Chapter 4 presents and discusses the results of this study. Chapter 5 discusses the significance and limitations of this study with a view to future improvements.

## CHAPTER 2

### FUNDAMENTALS OF CANINE GAIT

In order to understand how to map GRF data to subjective diagnostic scores using ANNs, the basic terminology and principles of canine gait and interpretation of GRF curves must be understood.

#### 2.1 TERMINOLOGY

This section summarizes the terminology used to describe a dog's coordinated and repetitive limb movement. Most of the terms used in this paper follow the guidelines suggested by Leach (1993). For notational convenience, each limb is expressed in terms of left or right and front or hind (i.e., LF, LH, RF, and RH).

##### 2.1.1 LIMB PAIRS

Limbs can be paired in three ways according to their relative position. Limbs on the same side of the body are *ipsilateral* (i.e., LF and LH or RF and RH). Limbs on opposite sides of the body across from each other are *contralateral* (i.e., LF and RF or LH and RH). Limbs on opposite sides of the body diagonal to each other are appropriately called *diagonal* limbs (i.e., LF and RH or RF and LH).

##### 2.1.2 TEMPORAL COMPONENTS OF GAIT

The *stance phase* is when a foot is on the ground, and the *swing phase* is when a foot is in the air. One *stride* equals to the stance and swing phases of one foot. A *gait cycle* occurs after each foot has moved once, and a *gait* occurs when the same gait cycle is repeated.

## 2.2 TYPES OF GAIT

Each gait type is characterized by the following three points: the sequence of footfalls during a gait cycle, the rhythm of footfalls, and the number of supporting paws at any given stance phase (Brown, 1986). Note that most named gaits have a range of variation. The most common canine gaits are the walk, the amble, the trot, the pace, the canter, and the gallop. The discussion in the following section is confined to the materials related to the trot, which is the gait used in this study.

### 2.2.1 FOOTFALL SEQUENCE AND SYMMETRICAL GAIT

The gait of a dog is commonly divided into two main groups, symmetrical and asymmetrical, according to footfall sequence. In a symmetrical gait, such as a walk, trot, or pace, the movement of the limbs on one side of the body repeats the movement of the limbs on the other side. In other words, ipsilateral feet are set down before either contralateral foot is set down, as shown in Figure 2.1. The order in which the paws are set on the ground are indicated by arrows. For example, if LH is set on the ground, then the following footfall sequence is LF, RH, RF, LH, and so on. Note that two or more adjacent feet in the diagram may be set down at the same time (i.e., LH with LF, LF with RH, RH with RF, RF with LH, or any three at a time).

In an asymmetrical gait, such as a canter or gallop, limb movements of on one side of the body do not repeat those of the other side. A more complete explanation of asymmetrical gaits is found in Brown (1986), Gray (1968), and Hollenbeck (1981).

### 2.2.2 RHYTHM OF FOOTFALLS AND NUMBER OF SUPPORTING LIMBS

Different types of symmetrical gaits can be distinguished by the relative time interval between the hind and front footfalls on one side. As mentioned above, the other side repeats the same motion.

A line chart of the rhythm on one side of a dog is shown in Figure 2.2 (Brown, 1986). For example, both feet on one side are set down at the same time when pacing. Therefore, the time interval between the hind and front footfalls is zero. In the trot, the diagonal legs move at the same time (i.e., RF with LH or LF with RH), which means that the time interval between footfalls on one side is 1/2 the time of one cycle. Depending on the rhythm of the footfalls, the number of paws on the ground at any given supporting phase differs, and usually there are only two supporting limbs at a time during a trot.

### 2.3 GRF CURVE

As shown in Figure 2.3, GRF can be divided into 3 vectors: vertical forces ( $F_z$ ), cranial-caudal forces ( $F_y$ ), and medial-lateral forces ( $F_x$ ). Forces applied in the direction of each vector shown in Figure 2.3 yield a positive GRF curve.

#### 2.3.1 GRF CURVE OF NORMAL TROT

GRF curves obtained from the limbs on one side of a healthy dog while trotting are plotted against the time of a single stride (Figure 2.4). The curves represent force applied, which is directly proportional to the acceleration of the dog in respective directions.<sup>1</sup> The first half of the curve is for the front limb, and the second half is for the ipsilateral hind limb. Points A and C correspond to the paw strikes of the front and hind limbs, respectively. Similarly, Points B and D correspond to the toe-offs of the front and hind limbs, respectively. Since the trot is a symmetrical gait, nearly identical curves can be obtained from the contralateral limbs in a healthy dog.

Each force has different clinical importance and implications. The vertical force ( $F_z$ ), which has the greatest magnitude, most directly measures the amount of weight a limb can bear. In general, front limbs bear more weight and function as the main supporting limbs. The cranial-caudal curve ( $F_y$ ) quantifies the forces that affect forward motion: braking force

---

<sup>1</sup>According to Newton's Second Law,  $F = ma$ , where  $F$  is force,  $m$  is mass, and  $a$  is acceleration

and propulsive force. The braking force indicates deceleration in the early stance phase when a paw is put on the plate; the propulsive force indicates the acceleration when the paw pushes off the ground. The front limbs mainly function to decelerate the dog while the hind limbs serve to accelerate the dog. As a result, the braking impulse<sup>2</sup> is greater in the front limbs while the propulsive impulse is generally greater in the hind limbs (Budsberg et al., 1987). The medial-lateral forces (Fx), which have the smallest magnitude, indicate lateral stability.

Most studies have used peak vertical forces, peak braking forces, peak propulsive forces, and associated impulses as discrete variables for analysis. Because of their small amplitude and large variation in a given dog and from dog to dog, medial-lateral forces have rarely been used in evaluating limb function. Limb-loading time or rate,<sup>3</sup> (Budsberg et al., 1988, 1995, 1996) weight distribution among the four limbs<sup>4</sup> (Budsberg et al, 1987), center of pressure, reaction torque, and applied moment of inertia have also been used in biomechanical analysis of canine gait to a limited extent (DeCamp, 1997).

### 2.3.2 GRF CURVE OF ABNORMAL TROT

GRF curves for all the limbs of a trotting dog before and after LH cranial cruciate ligament transection (CCLT) are superimposed for comparison in Figure 2.5 (vertical), Figure 2.6 (cranial-caudal), and Figure 2.7 (medial-lateral).

As shown in Figure 2.5 and Figure 2.6, the peak vertical, braking, and propulsive forces and associated impulses of the injured limb (LH) are lower than the preoperative values (Budsberg, 2001; DeCamp, 1997; Jevens et al., 1996; O'Connor et al., 1989; Rumph et al., 1995). The decrease in the peak vertical force of the injured limb indicates decreased weightbearing (Figure 2.5). The decrease in the peak braking and propulsive forces of the injured limb indicates reduced control over acceleration and deceleration (Figure 2.6). The

---

<sup>2</sup>Impulse is the total force applied over a stance phase.

<sup>3</sup>Time required from foot contact to reach peak magnitude (% of the complete stance phase).

<sup>4</sup>Weight distribution among the four limbs are calculated using the following formula: peak vertical force of a limb / sum of peak vertical forces of four limbs  $\times$  100.

decrease can be attributed not only to the mechanical joint instability induced by the surgery but also to the cartilage and meniscal injuries caused by that instability (Budsberg, 2001).

The diagonal (RF) and contralateral (RH) limb stance phase overlap indicates earlier placement of contralateral limb on the ground and protracted diagonal limb stance phase (Figure 2.5) in order to remove weight from the affected limb. Furthermore, lateral instability is more noticeable (Figure 2.7). The sharp increase in the peak medial-lateral force of the non-injured limb (LF in this case) indicates the dog's movement to compensate medial-lateral balance instability caused by the injured limb. Compensatory action by non-injured limbs is a reasonable way to explain the abnormal Post-CCLT curves in Figures 2.5–2.7. However, the redistribution of forces to the other three limbs when one limb is lame has not been completely understood (DeCamp, 1997). Several studies have suggested that lameness in a hind limb increases compensatory vertical loading of the contralateral limb (Budsberg, 2001; DeCamp, 1997; Jevens et al., 1996; Rumph et al., 1995). Changes in ipsilateral and contralateral front limb vertical force value have also been reported (Rumph et al., 1995). Another study reported a significant decrease in the ipsilateral front braking impulse and mentioned the possibility that force redistribution involves all four limbs, which results in GRF curve alterations in all directions (Jevens et al., 1996). It is likely that force redistribution is affected by many factors, including severity of lameness, cause of lameness, joints affected, duration of lameness, and the dog's neurological modification ability (Budsberg, 2001; DeCamp, 1997; Jevens et al., 1996 ).

### 2.3.3 GRF CURVE ALTERATION AND SUBJECTIVE SCORING SYSTEM

As mentioned above, alterations in the GRF of an injured limb and possibly the other limbs are associated with lameness. However, the variables found to be associated with lameness and the strength of correlation between GRF curves and subjective lameness scores have varied from study to study. Budsberg et al. (1987) and Jevens et al. (1996) found significant correlation between the peak vertical forces and impulses and subjective lameness scores.

In other studies, limb-loading time and weight distribution among four limbs corresponded with the clinical evaluation of improved weightbearing in the injured limb (Budsberg et al., 1988).

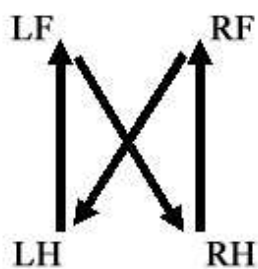


Figure 2.1: Footfall Sequence of Symmetrical Gait

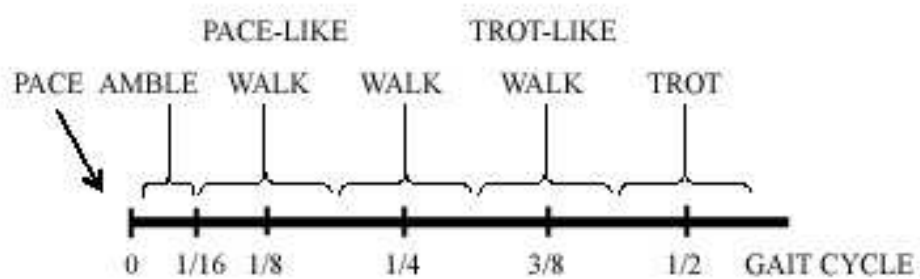


Figure 2.2: Rhythm of Footfalls in Symmetrical Gait

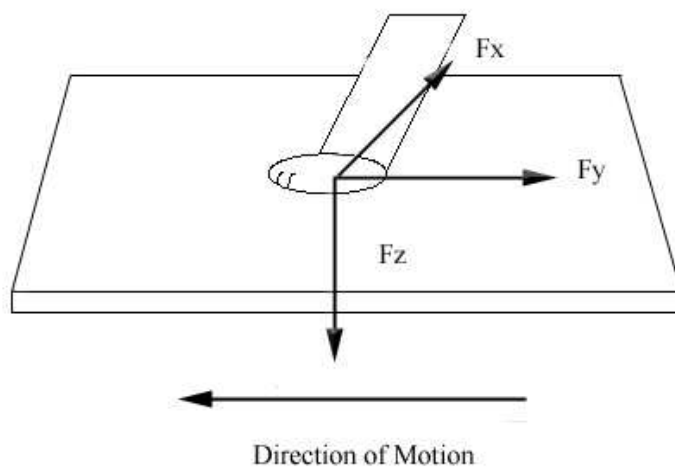


Figure 2.3: Orthogonal Components of GRF

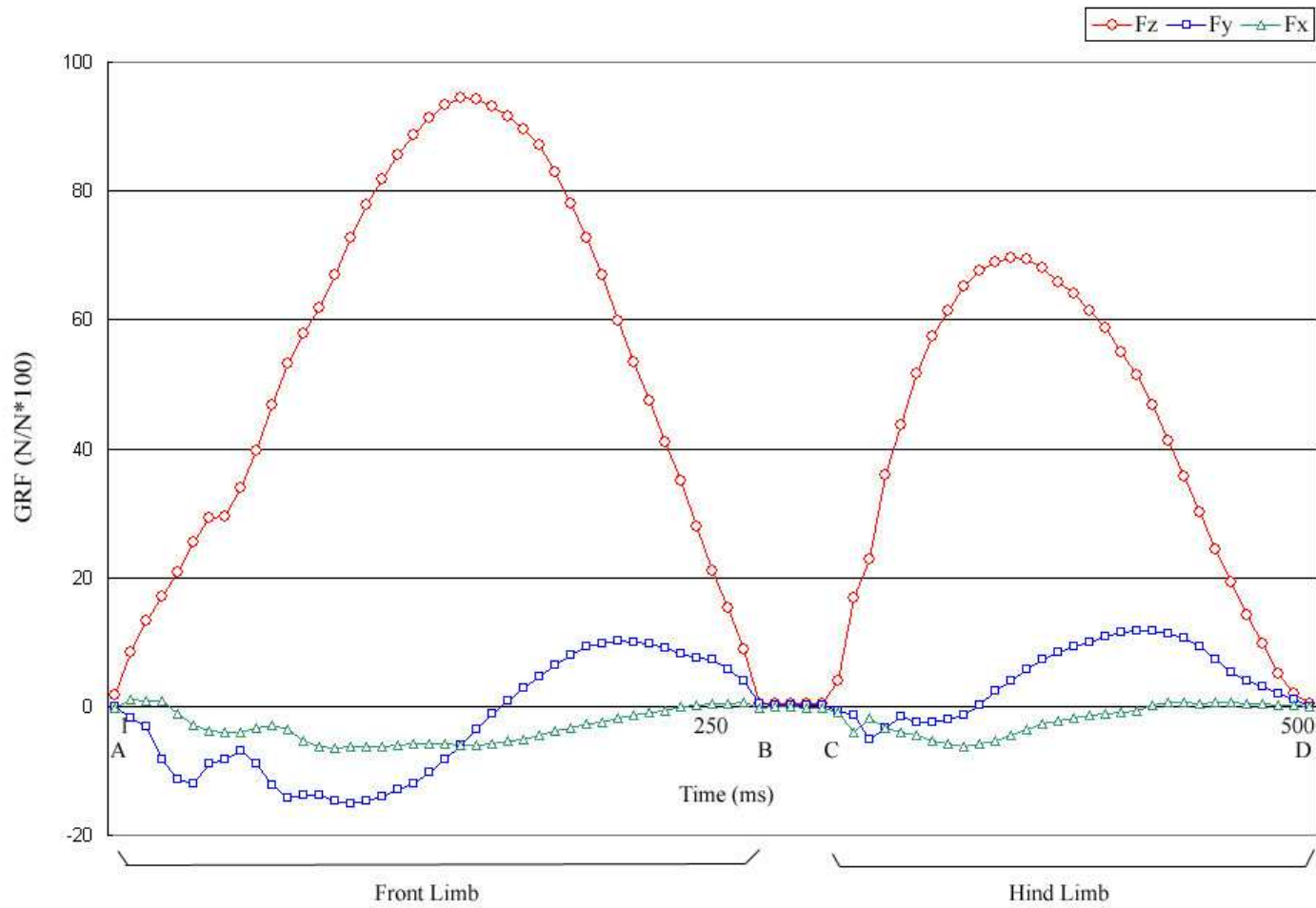


Figure 2.4: Representative GRF Curves of Normal Canine Gait

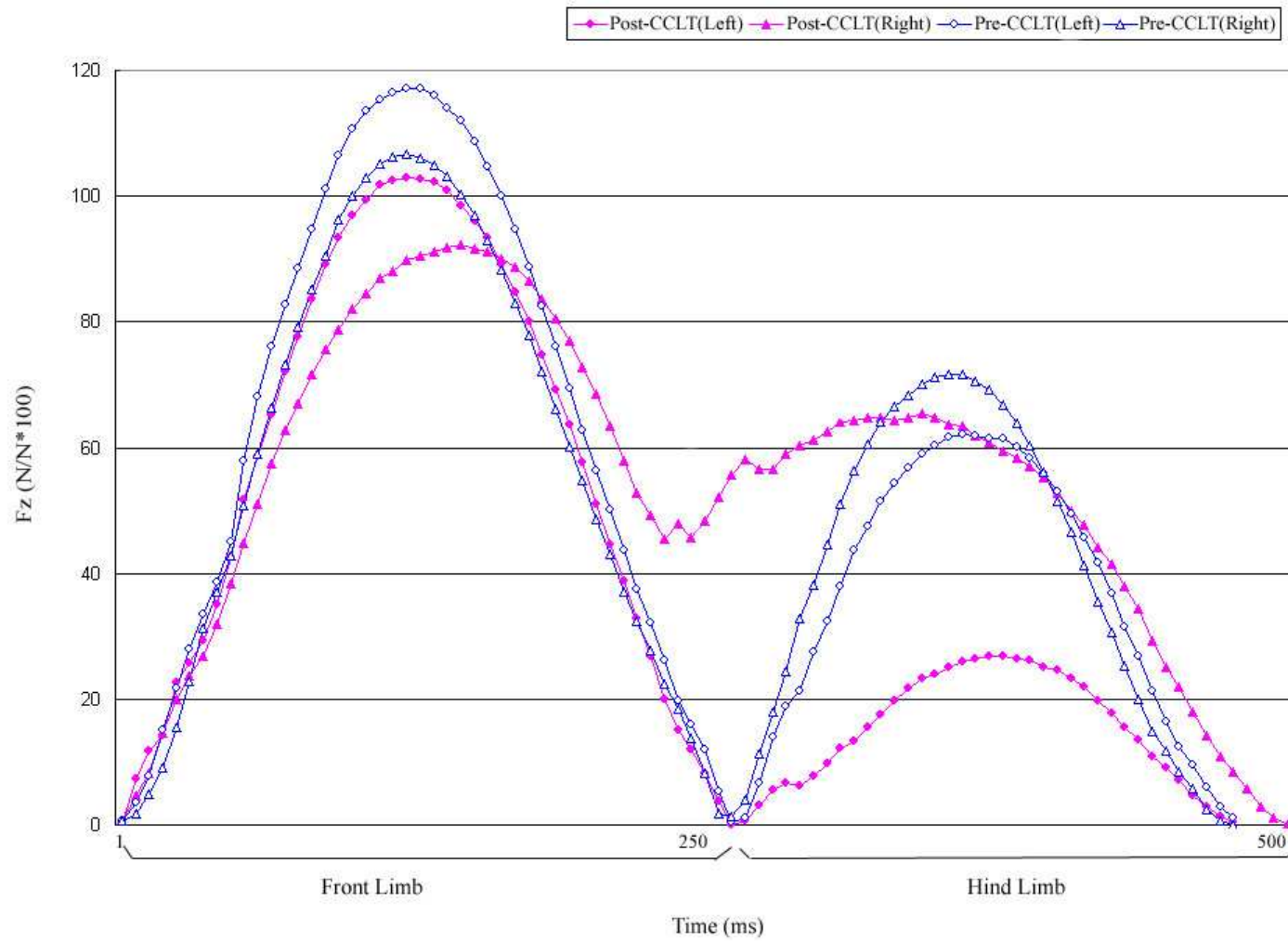


Figure 2.5: Representative Vertical GRF Curves of Normal and Abnormal Canine Gait

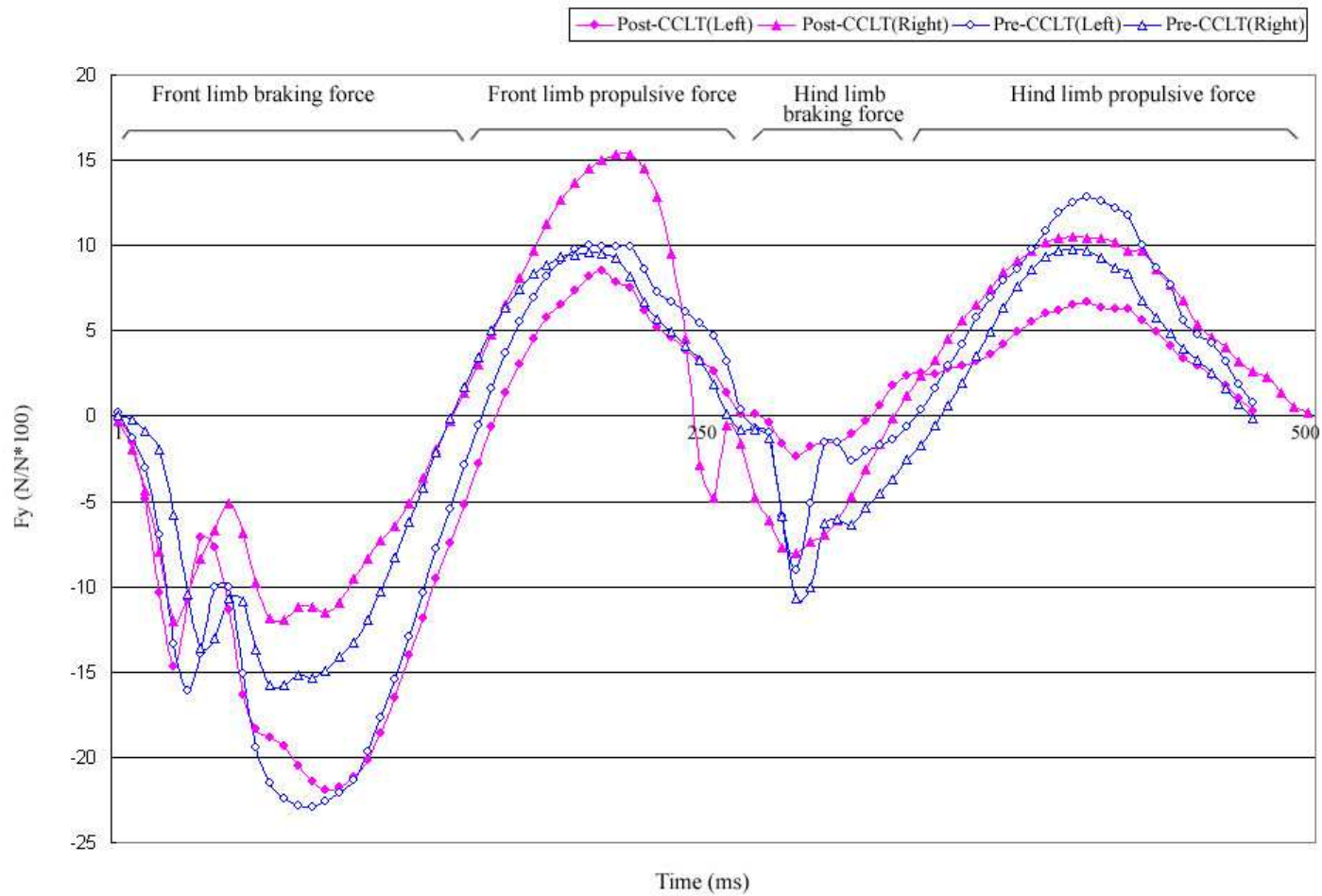


Figure 2.6: Representative Cranial-Caudal GRF Curves of Normal and Abnormal Canine Gait

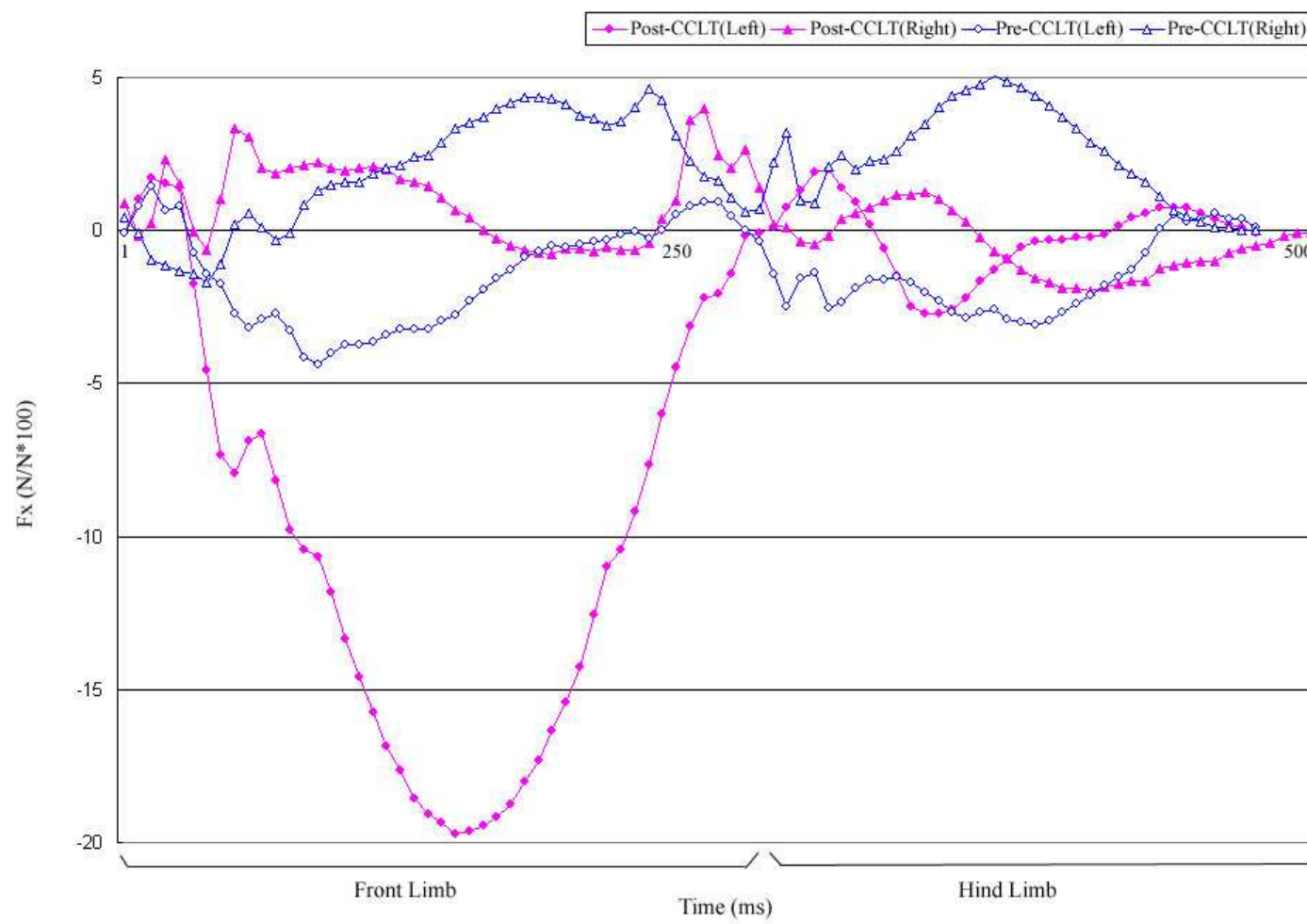


Figure 2.7: Representative Medial-Lateral GRF Curves of Normal and Abnormal Canine Gait

## CHAPTER 3

### METHODOLOGY

#### 3.1 DATA COLLECTION TOOLS AND PROCEDURE FOR THE PHARMACEUTICAL STUDY

Data gathered from force-plate analysis in an earlier pharmaceutical study of osteoarthritis drug development<sup>1</sup> were used in this study with ANNs to map variables extracted from GRF curves to subjective diagnostic score of lameness. Twenty-one institution-owned, clinically normal adult hound-type dogs (Dogs A–U) of mass from 19 to 32.2 *kg* (Avg. 24.36 *kg*) were used. Each dog underwent LH cranial cruciate ligament transection, inducing osteoarthritis in the knee (stifle) joint. GRF data were collected using two biomechanical force-plates flush with and in the center of a 12 meter walkway. Force-plates were interfaced with a computer system and GRFs were recorded at 1 millisecond intervals using Acquire 7.31 data acquisition software.<sup>2</sup> In addition, two photoelectric cells placed 2 meters apart were used to determine the velocity of the gait.

Without having access to force-plate test results, a veterinarian observed each dog and diagnosed the severity of lameness using the scoring system shown in Table 3.1. The lameness score indicates the abnormality in the movement of an injured limb during the stance phase as well as the swing phase. Subjective diagnostic scores were assigned by the veterinarian and GRF data were collected twice prior to and five times after the surgery. A total of seven different trials were conducted one month prior to ( $T_{-1}$ ), immediately prior to ( $T_0$ ), and one ( $T_1$ ), three ( $T_3$ ), six ( $T_6$ ), nine ( $T_9$ ), and twelve ( $T_{12}$ ) months after the surgery. For each trial, gait data of five valid attempts were collected from each dog, unless the subject was too lame

---

<sup>1</sup>The studies were approved by the Animal Care and Use Committee at the University of Georgia.

<sup>2</sup>Sharon Software, Inc., Dewitt, MI.

or distracted to perform the test. The GRF data were considered valid if the trot was at a velocity of 1.7 to 2.1  $m/s$  with acceleration variation within the range of  $-0.5$  to  $0.5 m/s^2$ .

### 3.2 DATA SET PREPARATION

The variables extracted from GRF curves for one gait attempt and the corresponding subjective lameness score were organized into a pattern,<sup>3</sup> and all the patterns acquired for the pharmaceutical study were organized into a data set.

A total of 678 patterns were obtained from the pharmaceutical study. For twelve dogs, data from five gait attempts were collected on seven different dates. For nine dogs, data from 1–5 gait attempts were collected on 5–7 different dates. A summary of the number of patterns obtained for each of the twenty-one dogs is shown in Table 3.2. As shown in Table 3.3, all the dogs had a lameness score of LM1 prior to the surgery ( $T_{-1}$  and  $T_0$ ), and all of them were diagnosed as lame (LM2 or LM3) one month after the surgery ( $T_1$ ). The lameness score of some dogs fluctuated after the surgery. Only nine dogs (Dogs A–I) received lameness scores of LM1, LM2, and LM3, whereas the rest of the dogs (Dogs J–U) received lameness scores of LM1 and LM2. None of the dogs received a score of LM4. A total of 265, 354, and 59 patterns for LM1, LM2, and LM3, respectively, were used (Table 3.4).

### 3.3 ANN DESIGN TOOL AND PROCEDURE

ANNs were developed using NeuroShell 2<sup>4</sup> to map a set of objective GRF variables to a corresponding subjective lameness score (LM1, LM2, or LM3).<sup>5</sup> This study focused on finding the preferred ANN models, single input variables, and sets of input variables.

---

<sup>3</sup>A pattern is a record of input variables and corresponding output target values from a single observation.

<sup>4</sup>Ward Systems Group, Inc., Frederic, MD.

<sup>5</sup>ANNs developed in this study only differentiated three classes of lameness because no dog received a lameness score of LM4 (Section 3.2).

### 3.3.1 ANN ARCHITECTURE AND MODELS

The standard 3-layer backpropagation networks (BPNs) and probabilistic neural networks (PNNs) were used because BPNs have been shown to be suitable for human and equine gait abnormality detection and PNNs have been shown to be suitable for classification problems and perform well with scarce data (Barton & Lees, 1997; Chau, 2001 [b]; Cheron, 2003; Hahn et al., 2005; Huang, 2004; Huang & Liao, 2004; Keegan et al., 2003; Lafuente et al., 1997; Saini et al., 2003; Schöllhorn, 2004; Schobesberger & Peham, 2002; Simon, 2004; Su & Wu, 2000; Wu et al., 2001; and Zhao et al., 2004). The three ANN models tested were (a) BPN with one output node (Figure 3.1), (b) BPN with three output nodes (Figure 3.2), and (c) PNN with three output nodes (Figure 3.3). ANN architecture parameters used in this study are listed in Table 3.5.

BPNs consist of three layers: input, hidden, and output layers. Each node in a particular layer is connected to all the nodes in adjacent layers. In other words, each network is fully connected. The number of input nodes is equal to the number of input variables used by the network. The number of output nodes depends on the classification strategy. One output node can be used to differentiate multiple classes or  $N$  output nodes can be used to differentiate  $N$  classes. The number of hidden nodes is arbitrary.

PNNs consist of four layers: input, pattern, summation, and output layers. The number of input nodes is equal to the number of input variables used by the network. The number of output nodes is equal to the number of classes ( $N$ ). The pattern layer contains  $N$  pools of pattern nodes, and the number of pattern nodes is equal to the number of patterns in the training data set. Each input node is connected to all the nodes in the pattern layer. Pattern nodes of  $N$ th pool are connected to the  $N$ th summation nodes (Specht, 1990).

### 3.3.2 INPUT VARIABLES

Inputs to each ANN were variables extracted from GRF curves (Tables 3.6–3.8 and Figures 3.4–3.7). The software used for data acquisition provided raw GRF data as well as the

following calculated variables: peak vertical force (PFz), peak braking force (PFy-b), peak propulsive force (PFy-p), peak medial-lateral force (PFx), associated impulses (IFz, IFy-b, and IFy-p), average rising (AveR) and falling slopes (AveF) of vertical forces, and time when the peak vertical force was reached (TFz) (Table 3.6 and Figures 3.4–3.6). Additional variables as shown in Table 3.7 were calculated using these variables. These variables were tested because they have been found to be associated with lameness in previous studies.

In addition, variables related to the Mid Point, which is the minimum point between the peak vertical forces of ipsilateral limbs (Table 3.8 and Figure 3.7), were calculated from the raw data. The Mid Point of the non-affected side of the dog (Mid[R]) is noticeably higher than the Mid Point of the affected side in an abnormal trot. Mid(R) seems to capture the various aspects of a dog's attempt to reduce weight on the injured limb. GRF curves for all the limbs of a trotting dog after LH Cranial Cruciate Ligament Transection (CCLT) are presented in Figure 3.8 to show the estimated cadence. At any given moment in an abnormal trot, either two diagonal feet or three total feet are touching the ground. For a dog to keep equilibrium during locomotion (as long as the vertical force is considered), the center of the gravity (G) must lie either on the diagonal line connecting the two feet on the ground or within the triangle of the three feet touching the ground. If a dog wants to remove weight from the injured limb (LH) and keep equilibrium, the center of gravity must be shifted to the right or to the front. In order to shift the center of gravity to the right of the intersection of the diagonal line, the contralateral limb (RH) must be set on the ground while the injured limb (LH) and the diagonal limb (RF) are on the ground. On the other hand, in order to shift the center of gravity to the front of the intersection of the diagonal line, the diagonal limb (RF) must be carried way behind until the ipsilateral limb (LF) is set on the ground. As shown in Figure 3.8, the dog accomplishes this shift in center of gravity by setting down the contralateral limb (RH) earlier and by elongating the stance phase of the diagonal limb (RF). Since the trot is a symmetrical gait, the difference in magnitude of the Mid Point

for each side of the dog (Mid[R-L]) also can be a good indicator for distinguishing levels of lameness severity.

The magnitude of the Mid Points is affected by three factors: (a) front and hind limb stance phase overlap, (b) the falling slope of the front limb (AveF[LF] or AveF[RF]), which is affected by the peak vertical force of the front limb (PFz[LF] or PFz[RF]) and the duration of weightbearing once the peak vertical force is reached (TotalT[RF]-TFz[RF] or TotalT[LF]-TFz[LF]), and (c) the rising slope of the hind limb (AveR[LH] or AveR[RH]), which is affected by the peak vertical force of the hind limb (PFz[LH] or PFz[RH]) and the duration of weightbearing until the peak vertical force is reached (TFz[LH] or TFz[RH]). Therefore, Mid(R) and Mid(R-L) normalized by the sum of the peak vertical forces of any set of limbs that can be set on the ground simultaneously (i.e., two front limbs, two rear limbs, two diagonal limbs, any combinations of three limbs, and all the limbs) were also tested.

Note that the peak vertical force of the non-injured hind limb (RH) provided by the software was not precise enough. If the Mid Point was higher than 33% of the peak vertical force of the front limb (RF) as shown in Figure 3.7, the peak vertical force of the non-injured hind limb (RH) was calculated as 0. Hence, the peak vertical force of the non-injured limb (RH) was re-calculated.

### 3.3.3 TARGET VALUES AND INTERPRETATION OF ANN OUTPUT

Outputs of each ANN were lameness scores corresponding to those assigned by a veterinarian (LM1, LM2, and LM3). The target value coding procedure differed according to the ANN model used. For BPNs with one output node, the target values of LM1, LM2, and LM3 patterns were 0.1, 0.5, and 0.9, respectively (Table 3.9). For BPNs with three output nodes, the target values of LM1 patterns were 0.9, 0.1, and 0.1 for the nodes corresponding to LM1, LM2, and LM3, respectively (Table 3.10). Likewise, for the LM2 patterns and LM3 patterns, the target value for the corresponding node was 0.9 (0.1 for the other two nodes). For PNNs with three output nodes, the target values of LM1 patterns were 1, 0, and 0 for

the nodes corresponding to LM1, LM2, and LM3, respectively (Table 3.11). Likewise, for the LM2 patterns and LM3 patterns, the target value for the corresponding node was 1 (0 for the other two nodes).

The network output interpretation procedure differed according to the ANN model used. The output value of BPNs with one output node was interpreted as LM1, LM2, or LM3 if it was in the range of 0.1–0.35, 0.35–0.65, or 0.65–0.9, respectively. The output value of BPNs with three output nodes was interpreted as LM1, LM2, or LM3 when the corresponding node had the highest network output value. The output value of PNNs was interpreted as LM1, LM2, or LM3 if the binary output value of the corresponding node was 1.

### 3.3.4 ANN MODEL DEVELOPMENT AND EVALUATION

In order to develop and evaluate BPNs, a data set was divided into three mutually exclusive subsets: training, testing, and evaluation data sets. Each network was trained using the training data set. The testing data set was used to determine when the training should be terminated. If a network is trained until errors on a training data set are minimized, the network might learn either noise or features peculiar to the training data set in addition to the important features. In this study, the generalization ability of each model was checked periodically during training (i.e, every 200 training patterns presented) using the testing data set in order to prevent over-training. This process was repeated until the errors on the testing data set were reasonably minimized (i.e, no improvement was found on the testing data set after presenting 20000 training patterns since the best network had been found). Once the model was developed, patterns in the evaluation data set were presented to the trained network in order to evaluate how well the model generalized on a new set of data.

In order to develop and evaluate PNNs, a data set was divided into two mutually exclusive subsets: training and evaluation data sets. Each network was trained using the training data set. The input nodes received input values. Pattern nodes received the weighted sum of these inputs and calculated an activation level using the Gaussian function. The summation nodes

added all the inputs from the pattern nodes associated with that class. The output of the PNN result corresponded to the results of a probability density function. The results were of two kinds: binary output (0 or 1) and a value indicating the probability of each pattern belonging to a particular class. Unlike BPNs, each PNN required each training pattern to be presented to the network only once during training.

The only required control factor for a PNN was the smoothing factor. The smoothing factor determined the radial deviation of the Gaussian function. If the smoothing factor was too small, the networks did not generalize well on the new data set. If the smoothing factor was too large, the networks failed to learn the subtle relationships between inputs and outputs. In preliminary runs, a data set was divided into mutually exclusive 3 subsets (i.e., training, testing, and evaluation data sets) in order to choose appropriate smoothing factors. A testing data set was used to find the smoothing factor that produced fewer classification errors. Once the optimal smoothing factor was found, patterns from the testing data set were added to the training data set, and the PNN was retrained using the updated training data set. Once the model was developed, patterns in the evaluation data set were presented to the trained network in order to evaluate how well the model generalized on a new set of data.

The networks were developed using patterns from two-thirds of the dogs (14) in the data set and evaluated with patterns from the remaining dogs (7). In order to obtain results that better indicated model performance in clinical practice, the accuracy of each model was tested using an evaluation data set that never contained patterns from the same dog as patterns used in model development. Two different data sets (Data Configurations 1 and 2) were created. Because there were only nine dogs that received a lameness score of LM3 (Table 3.4), each evaluation data set contained three dogs with LM3 patterns and four other dogs. In Data Configuration 1, patterns from Dogs A–F, J–N, and P–R were used for model development, and patterns from Dogs G–I, O, and S–U were used for model evaluation (Table 3.12). In Data Configuration 2, patterns from Dogs D–I and N–U were used for model

development, and patterns from Dogs A-C and J-M were used for model evaluation. The number of patterns in each subset is presented in Table 3.13.

### 3.3.5 ANN MODEL ASSESSMENT

Once an ANN was trained and the results from the evaluation data set were obtained, a predicted lameness score was assigned to each pattern in the evaluation data set using the criteria given in Section 3.3.3. Each ANN was assigned an Overall Accuracy (OA), which is the sum of the patterns classified on the same level assigned by the veterinarian divided by the total number of patterns in the evaluation data set:

$$\text{OA} = \frac{a + b + c}{P} \times 100,$$

where  $a$  is the number of patterns in the evaluation data set classified as LM1 by the ANN and actually assigned LM1 by the veterinarian,  $b$  is the number of patterns in the evaluation data set classified as LM2 by the ANN and actually assigned LM2 by the veterinarian,  $c$  is the number of patterns in the evaluation data set classified as LM3 by the ANN and actually assigned LM3 by the veterinarian, and  $P$  is the number of patterns in the evaluation data set.

### 3.3.6 INPUT VARIABLES AND ANN MODEL SELECTION PROCEDURE

In order to identify the input variables that correlated well with lameness scores, the BPN with one output node was used with Data Configuration 1. The variables shown in Tables 3.6–3.8 were mapped by each ANN model individually. Various combinations of the input variables found to be useful were then used to create additional ANNs. If the multiple inputs increased the accuracy of the network, these variables, along with other input variables, were used to develop additional ANNs. If the accuracy was lower with the multiple inputs, alternative combinations were tested. After this process was repeated, unnecessary input variables were eliminated, and useful variables were kept for subsequent model development. Several ANNs were developed to examine the impact of a particular input variable on the accuracy.

Trial and error was used to a large extent because, typically, a veterinarian trained in orthopedics can differentiate the severity based on his experience but cannot provide a conclusive point of reference for the diagnosis. Once the promising sets of input variables were identified, input analysis was conducted for three ANN models using both data configurations. The accuracy of three ANN models was compared and the preferred set of input variables were selected based on the results obtained from both data configurations. In addition, the preferred number of hidden nodes for BPNs was determined using the preferred set of input variables.

Table 3.1: Subjective Scoring System

---

Lameness Score	Description
1	Trots normally
2	Slight lameness at trot
3	Moderate lameness at trot
4	Severe lameness at trot

---

Table 3.2: Number of Patterns Acquired at Every Observation Point

<b>Dog</b>	<b>Number of Patterns</b>							<b>Total</b>
	<b>T<sub>-1</sub></b>	<b>T<sub>0</sub></b>	<b>T<sub>1</sub></b>	<b>T<sub>3</sub></b>	<b>T<sub>6</sub></b>	<b>T<sub>9</sub></b>	<b>T<sub>12</sub></b>	
A	5	5	5	5	5	5	5	35
B	5	5	5	5	5	5	5	35
C	5	5	5	4	0	5	5	29
D	5	5	5	5	5	5	5	35
E	5	5	4	5	5	5	5	34
F	5	5	0	5	5	5	5	30
G	5	5	0	0	5	1	5	21
H	5	5	2	5	5	5	5	32
I	5	5	0	1	5	2	0	18
J	5	5	5	5	5	5	5	35
K	5	5	5	5	5	5	5	35
L	5	5	1	5	5	5	5	31
M	5	5	5	5	5	5	5	35
N	5	5	5	5	5	5	5	35
O	5	5	0	5	5	5	5	30
P	5	5	5	5	5	5	5	35
Q	5	5	5	5	5	5	5	35
R	5	5	5	5	5	5	5	35
S	5	5	5	5	5	5	5	35
T	5	5	3	5	5	5	5	33
U	5	5	5	5	5	5	5	35
<b>Total</b>	105	105	75	95	100	98	100	678

Table 3.3: Score Obtained for Each Dog at Each Observation Point

Dog	Lameness Score						
	T <sub>-1</sub>	T <sub>0</sub>	T <sub>1</sub>	T <sub>3</sub>	T <sub>6</sub>	T <sub>9</sub>	T <sub>12</sub>
A	1	1	3	2	2	2	3
B	1	1	3	2	2	2	2
C	1	1	3	2	*	2	2
D	1	1	3	3	2	2	2
E	1	1	3	2	2	1	2
F	1	1	*	3	2	2	2
G	1	1	*	*	3	3	2
H	1	1	3	3	3	1	2
I	1	1	*	2	2	3	*
J	1	1	2	2	2	2	2
K	1	1	2	2	2	2	2
L	1	1	2	2	2	2	1
M	1	1	2	1	1	1	1
N	1	1	2	2	2	2	2
O	1	1	*	2	2	2	1
P	1	1	2	2	1	2	2
Q	1	1	2	2	2	2	2
R	1	1	2	2	1	2	2
S	1	1	2	2	2	1	2
T	1	1	2	2	2	2	2
U	1	1	2	2	2	2	2

\* No score available

Table 3.4: Number of Patterns Acquired for Each Dog

<b>Number of Patterns</b>				
<b>Dog</b>	<b>LM1</b>	<b>LM2</b>	<b>LM3</b>	<b>Total</b>
A	10	15	10	35
B	10	20	5	35
C	10	14	5	29
D	10	15	10	35
E	15	15	4	34
F	10	15	5	30
G	10	5	6	21
H	15	5	12	32
I	10	6	2	18
J	10	25	0	35
K	10	25	0	35
L	15	16	0	31
M	30	5	0	35
N	10	25	0	35
O	15	15	0	30
P	15	20	0	35
Q	10	25	0	35
R	15	20	0	35
S	15	20	0	35
T	10	23	0	33
U	10	25	0	35
<b>Total</b>	265	354	59	678

Table 3.5: ANN Architecture Parameters

<b>BPN</b>	<b>Value</b>
Number of Oupptput Nodes	1 or 3
Number of Input Nodes	Varied
Number of Hidden Nodes	2
Learning Rate	0.1
Momentum	0.1
Initial Weight	0.3
Activation Function (Input Layer)	Linear
Activation Function (Hidden Layer)	Logistic
Activation Function (Output Layer)	Logistic

---

<b>PNN</b>	<b>Value</b>
Number of Oupptput Nodes	3
Number of Input Nodes	Varied
Number of Hidden Nodes	290, 474 (Data Configuration 1) 268, 443 (Data Configuration 2)
Activation Function	Gaussian

Table 3.6: Input Variables Provided by the Software

<b>Input Variables</b>	<b>Notation</b>
Peak vertical forces	PFz
Vertical impulses	IFz
Time when peak vertical forces are reached	TFz
Average rising slopes of vertical forces	AveR
Average falling slopes of vertical forces	AveF
Total duration of stance phase	TotalT
Peak braking forces	PFy-b
Braking impulses	IFy-b
Peak propulsive forces	PFy-p
Propulsive impulses	IFy-p
Peak medial-lateral forces	PFx

Table 3.7: Input Variables Calculated from the Variables Listed in Table 3.6

<b>Input Variables</b>	<b>Notation</b>
Peak vertical force differences between the injured side of the dog	PFz(LF-LH)
the non-injured side of the dog	PFz(RF-RH)
the two front limbs	PFz (RF-LF)
the two hind limbs	PFz (RH-LH)
Percentage of weightbearing in injured limb (PFz[LH] normalized by sum of the PFz of all the limbs)	WB
Duration of front limb stance phase after the PFz is reached	TotalT(RF)-TFz(RF) TotalT(LF)-TFz(LF)

Table 3.8: Input Variables Calculated from the Raw Data

<b>Input Variables</b>	<b>Notation</b>	<b>Normalized by</b>
Mid Points	Mid(R)	
	Mid(R)/FRONT	PFz(RF)+PFz(LF)
	Mid(R)/HIND	PFz(RH)+PFz(LH)
	Mid(R)/PFz(RF+LH)	PFz(RF)+PFz(LH)
	Mid(R)/PFz(LF+RH)	PFz(LF)+PFz(RH)
	Mid(R)/PFz(RIGHT)	PFz(RF)+PFz(RH)
	Mid(R)/PFz(LEFT)	PFz(LF)+PFz(LH)
	Mid(R)/PFz(RF+LF+LH)	PFz(RF)+PFz(LF)+PFz(LH)
	Mid(R)/PFz(RH+LF+LH)	PFz(RH)+PFz(LF)+PFz(LH)
	Mid(R)/PFz(RF+RH+LH)	PFz(RF)+PFz(RH)+PFz(LH)
	Mid(R)/PFz(RF+RH+LF)	PFz(RF)+PFz(RH)+PFz(LF)
	Mid(R)/PFz(ALL)	PFz(RF)+PFz(RH)+ PFz(LF)+PFz(LH)
Mid Points difference	Mid(R-L)	
	Mid(R-L)/FRONT	PFz(RF)+PFz(LF)
	Mid(R-L)/HIND	PFz(RH)+PFz(LH)
	Mid(R-L)/PFz(RF+LH)	PFz(RF)+PFz(LH)
	Mid(R-L)/PFz(LF+RH)	PFz(LF)+PFz(RH)
	Mid(R-L)/PFz(RIGHT)	PFz(RF)+PFz(RH)
	Mid(R-L)/PFz(LEFT)	PFz(LF)+PFz(LH)
	Mid(R-L)/PFz(RF+LF+LH)	PFz(RF)+PFz(LF)+PFz(LH)
	Mid(R-L)/PFz(RH+LF+LH)	PFz(RH)+PFz(LF)+PFz(LH)
	Mid(R-L)/PFz(RF+RH+LH)	PFz(RF)+PFz(RH)+PFz(LH)
	Mid(R-L)/PFz(RF+RH+LF)	PFz(RF)+PFz(RH)+PFz(LF)
	Mid(R-L)/PFz(ALL)	PFz(RF)+PFz(RH)+ PFz(LF)+PFz(LH)

Table 3.9: Target Value Coding (BPN with One Output Node)

Lameness Score	Target Value
	Output Node
LM1	0.1
LM2	0.5
LM3	0.9

Table 3.10: Target Value Coding (BPN with Three Output Nodes)

Lameness Score	Target Value		
	Output Node 1	Output Node 2	Output Node 3
LM1	0.9	0.1	0.1
LM2	0.1	0.9	0.1
LM3	0.1	0.1	0.9

Table 3.11: Target Value Coding (PNN with Three Output Nodes)

Lameness Score	Target Value		
	Output Node 1	Output Node 2	Output Node 3
LM1	1	0	0
LM2	0	1	0
LM3	0	0	1

Table 3.12: Two Data Configurations

<b>Data Configuration</b>	<b>Dogs in Model Development</b>	<b>Dogs in Model Evaluation</b>
1	A-F, J-N, P-R	G-I, O, S-U
2	D-I, N-U	A-C, J-M

Table 3.13: Number of Patterns in Data Configurations 1 and 2

<b>Data Configuration 1</b>	<b>LM1</b>	<b>LM2</b>	<b>LM3</b>	<b>Total</b>
Training	110	157	23	290
Testing	70	98	16	184
Evaluation	85	99	20	204
Total	265	354	59	678

<b>Data Configuration 2</b>	<b>LM1</b>	<b>LM2</b>	<b>LM3</b>	<b>Total</b>
Training	103	142	23	268
Testing	67	92	16	175
Evaluation	95	120	20	235
Total	265	354	59	678

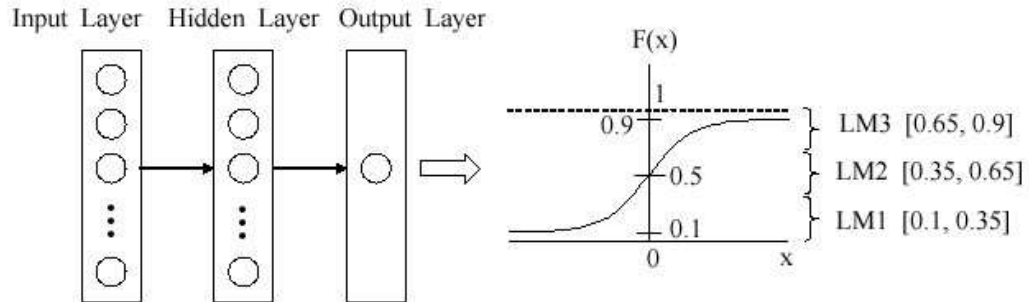


Figure 3.1: BPN with One Output Node to Differentiate Three Classes

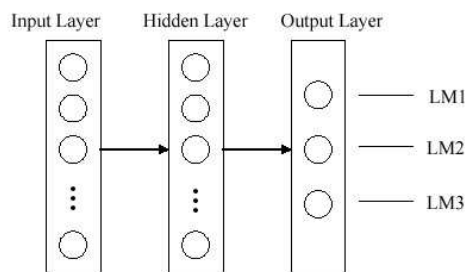


Figure 3.2: BPN with Three Output Nodes to Differentiate Three Classes

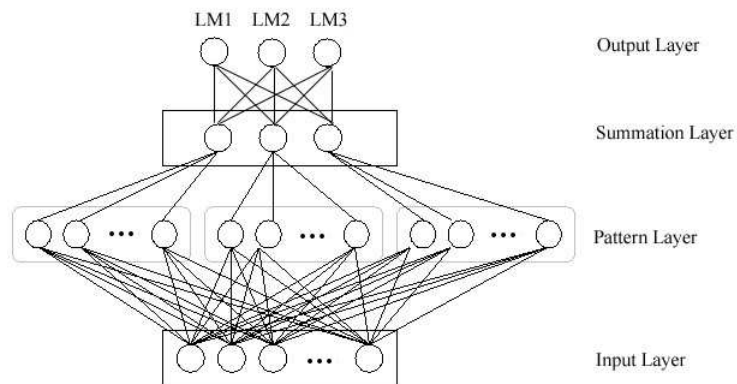


Figure 3.3: PNN with Three Output Nodes to Differentiate Three Classes

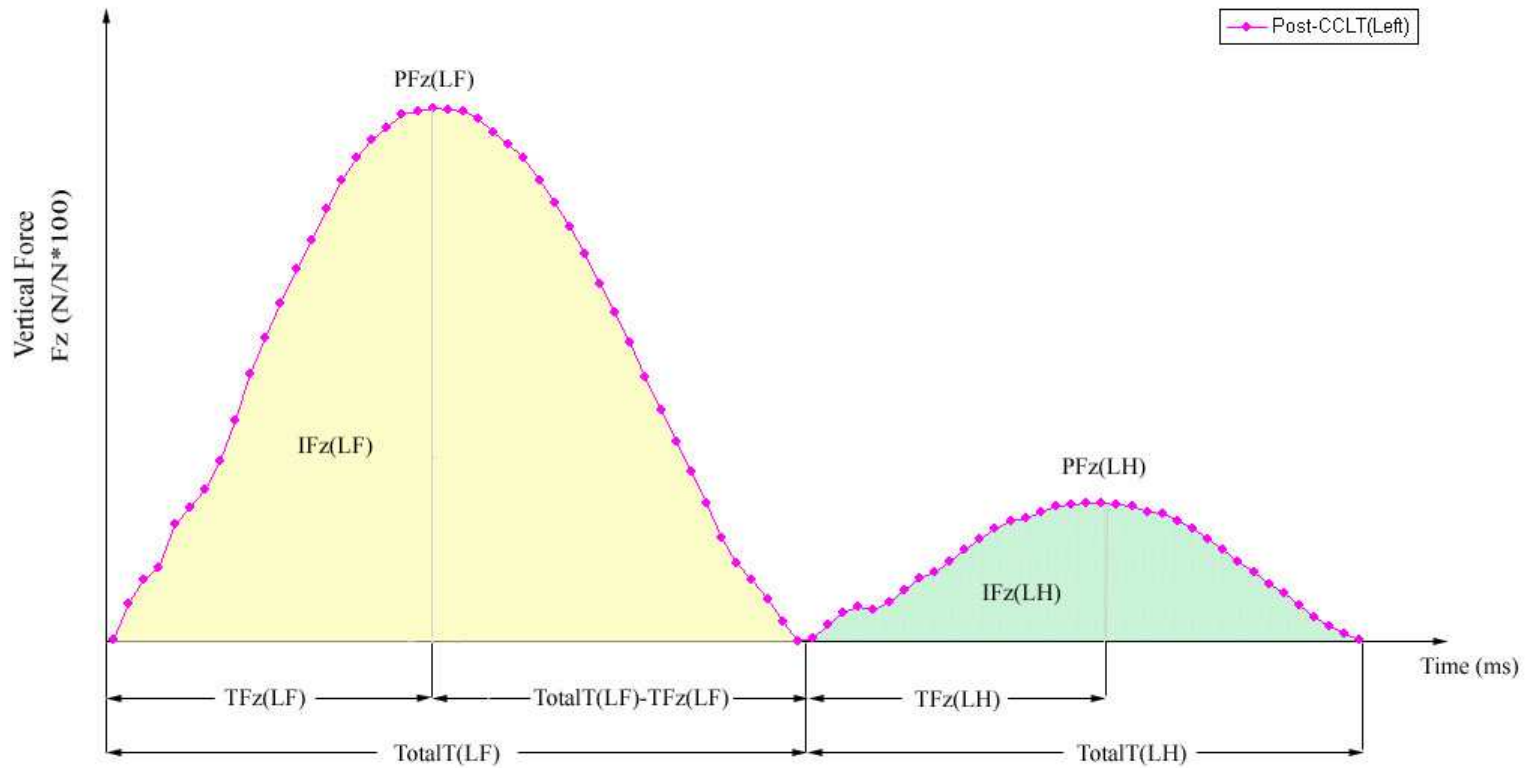


Figure 3.4: Vertical GRF Input Variables

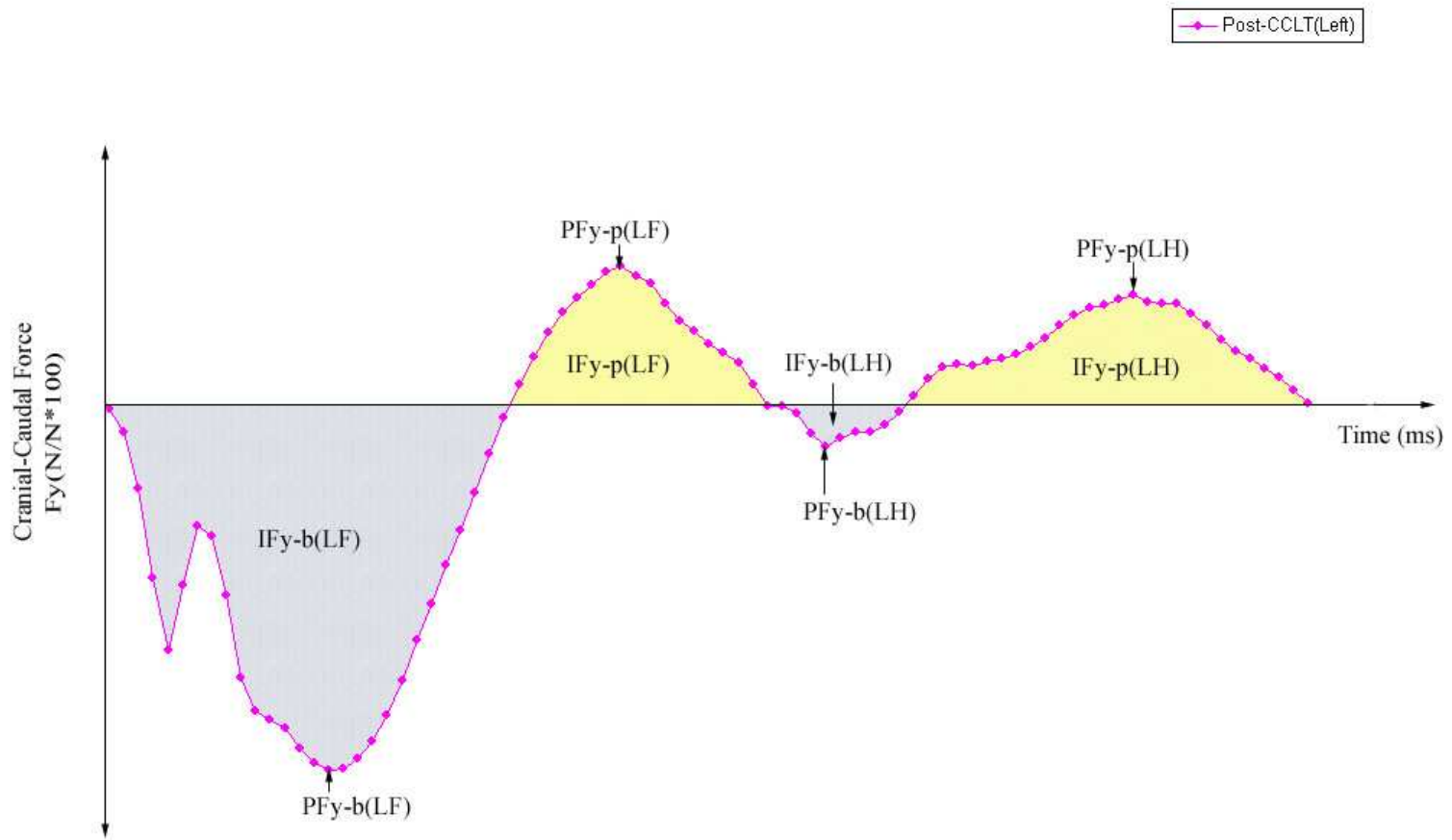


Figure 3.5: Cranial-Caudal GRF Input Variables

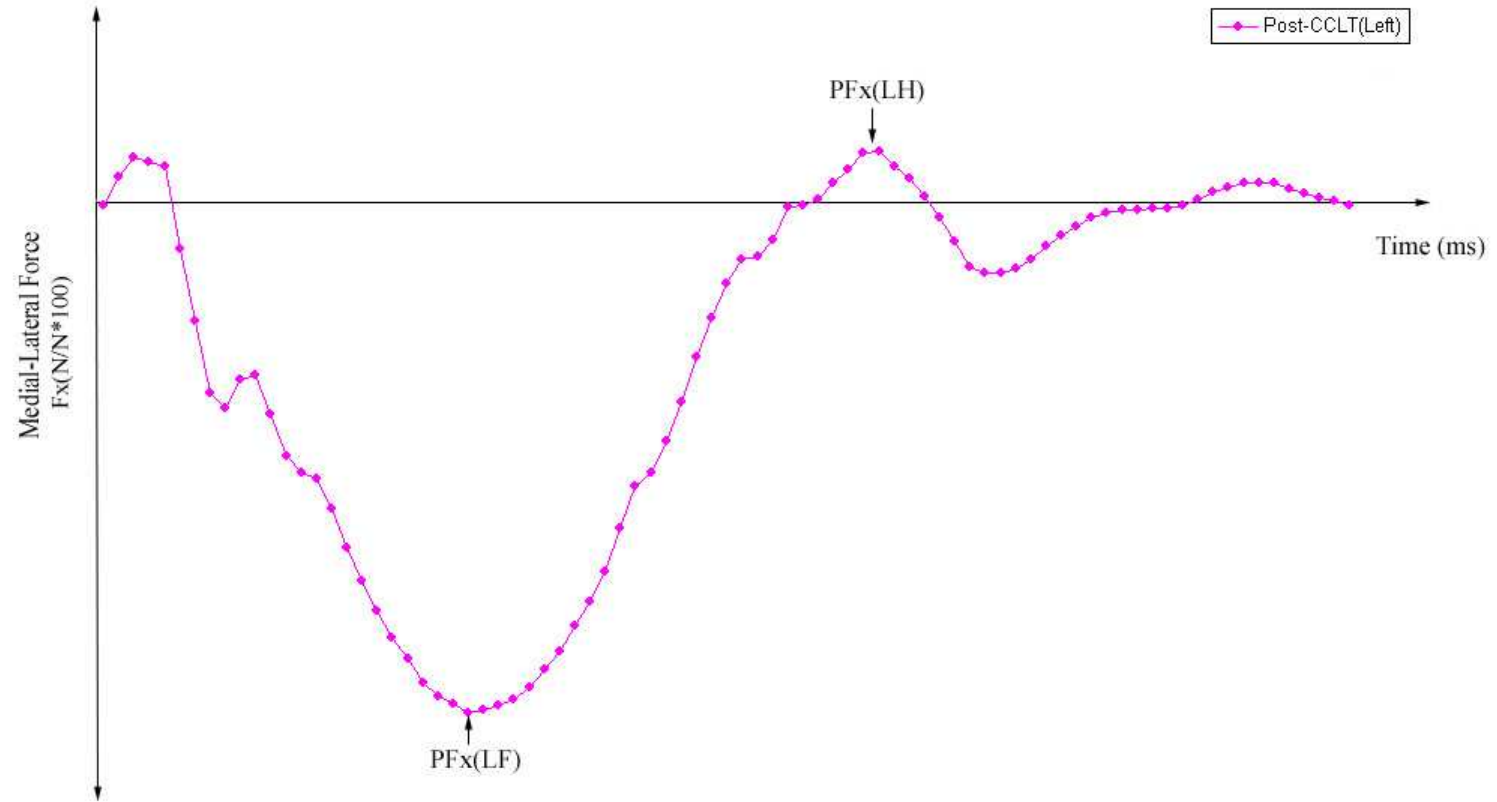


Figure 3.6: Medial-Lateral GRF Input Variables

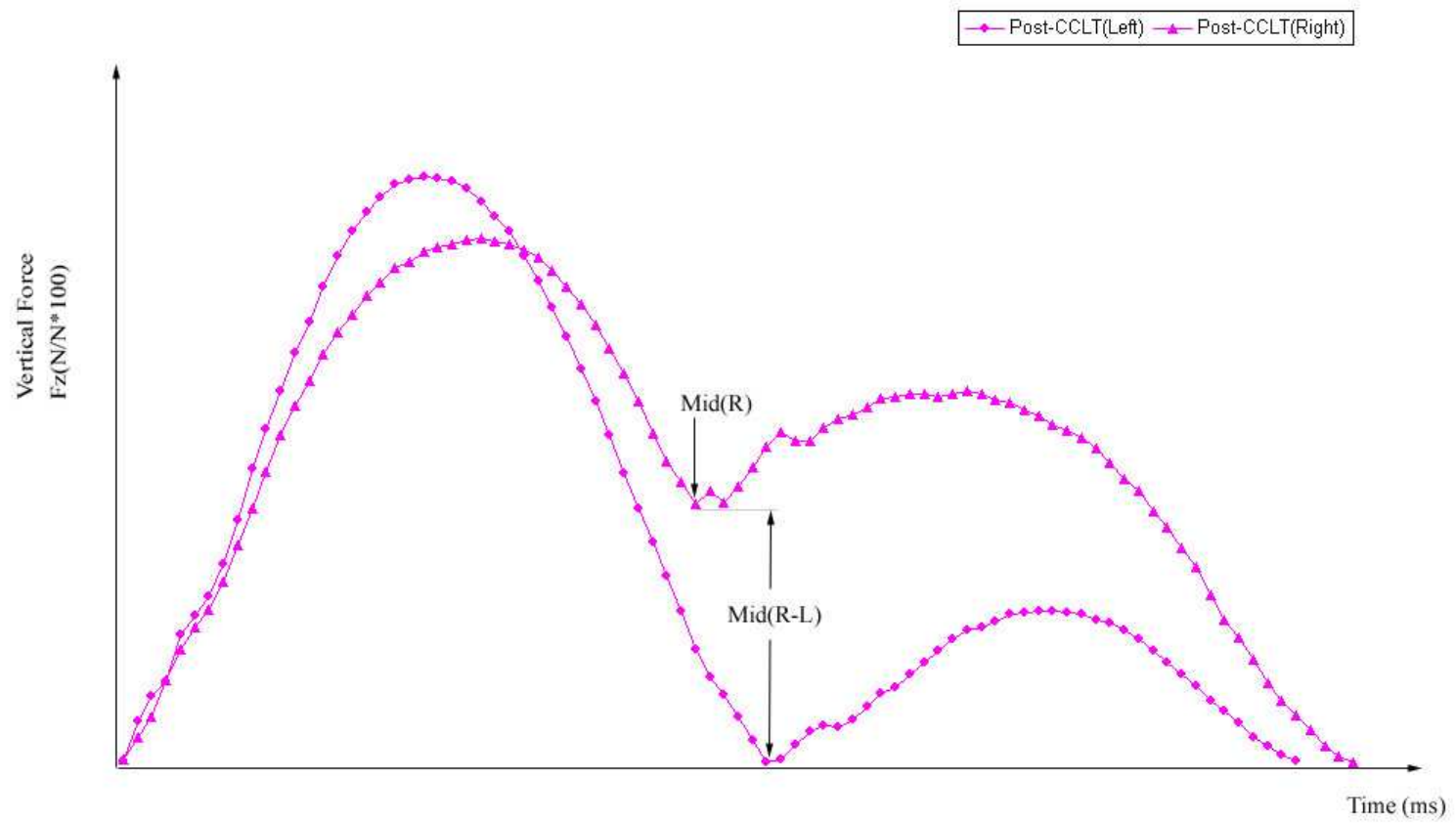


Figure 3.7: Input Variables Related to Mid Point

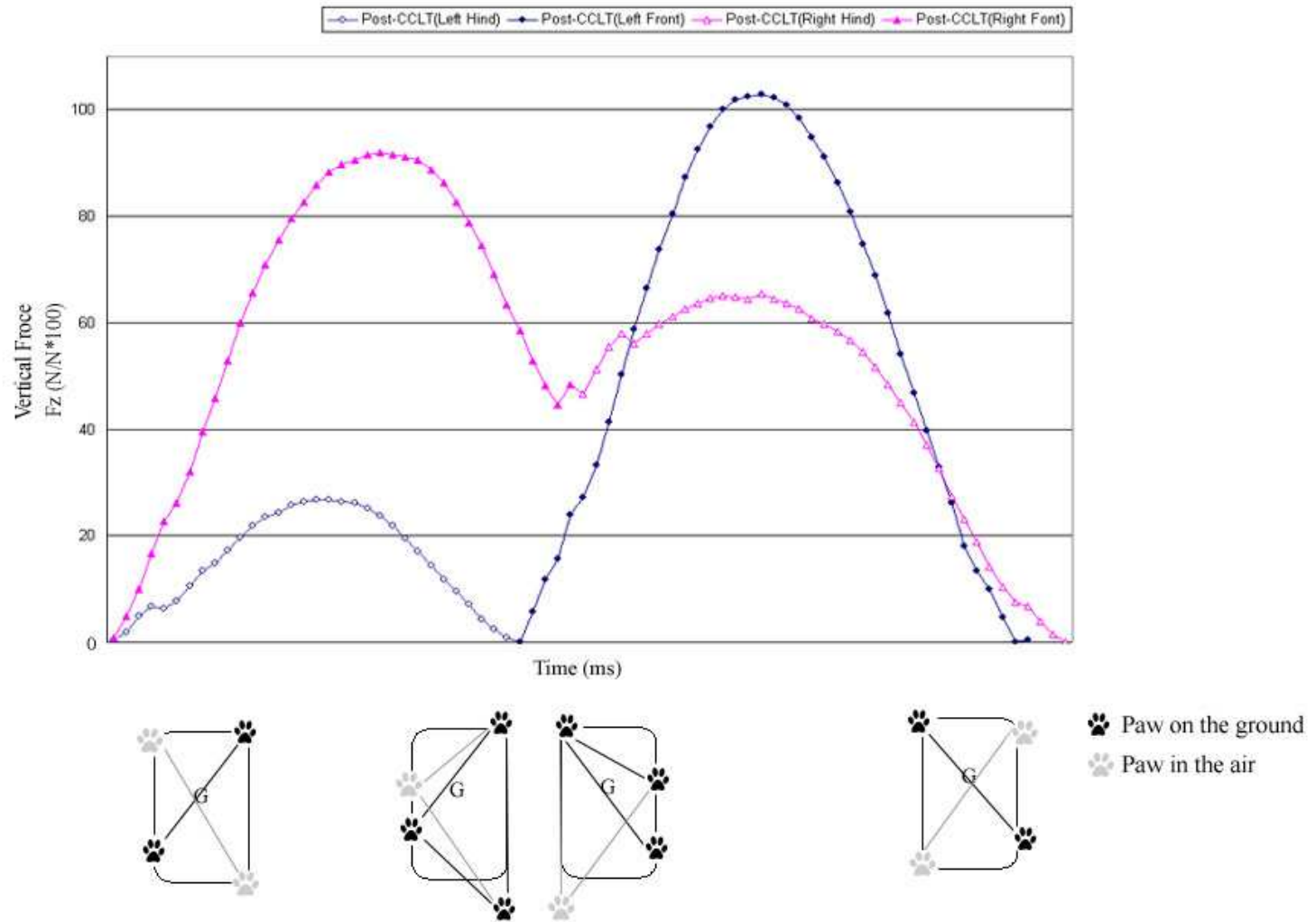


Figure 3.8: Shift in Center of Gravity during Abnormal Gait

## CHAPTER 4

### RESULTS AND DISCUSSION

#### 4.1 PRELIMINARY INPUT ANALYSIS AND IMPORTANT SINGLE INPUT VARIABLES

The results obtained from ANNs using the single input variables commonly used for other canine studies are shown in Table 4.1. None of the conventional variables produced acceptable levels of accuracy (39.2–64.7%). The results obtained from ANNs using single input variables suggested in this study are shown in Table 4.2. ANNs using Mid(R-L)/FRONT, Mid(R-L)/HIND, or Mid(R-L)/LEFT distinguished three lameness classes with an accuracy of 93.6%, 90.7%, and 90.7%, respectively, while the accuracy of ANNs using other input variables was in the range of 55.4–63.7%. Neither the Mid Point of the non-affected side of the dog (Mid[R]) nor the difference in magnitude of the Mid Point for each side of the dog (Mid[R-L]) alone differentiated three lameness classes or distinguished normal from abnormal gait that well (Table 4.2). The difference had to be normalized by the sum of the peak vertical forces of the two front limbs, two hind limbs, or two left limbs in order to produce an accuracy above 90%.

When Mid(R-L)/FRONT and Mid(R-L)/HIND were used together, the accuracy of the model improved 2–5% (Table 4.3). Using other combinations of these three input variables, ANNs performed 2–7% worse than the ANN using Mid(R-L)/FRONT and Mid(R-L)/HIND. When other single variables were used by the ANN in combination with Mid(R-L)/FRONT and Mid(R-L)/HIND, model accuracy did not improve except when PFz(LF) was used as well (Table 4.4). However, when multiple input variables were used in combination with these two variables, the accuracy improved slightly. The highest accuracy of 96.6% was obtained when peak vertical forces of RF and RH, average falling slope of RF, and average rising slope

of RH were used along with Mid(R-L)/FRONT and Mid(R-L)/HIND. When other single variables were used in combination with these six variables, model accuracy decreased.

## 4.2 SELECTION OF PREFERRED ANN MODEL AND SETS OF INPUT VARIABLES

After the preliminary input variable analysis, limited input analysis was done for all the ANN models and data configurations. Additional input analysis and testing on the other data configuration was performed to determine if input variables found to be useful on one set of dogs would generalize well on data from other dogs. Nine sets of input variables were tested (Table 4.5).

### 4.2.1 ANN MODEL COMPARISON

Using the nine sets of input variables with Data Configuration 1, the ANNs differentiated three classes of lameness 87.8% to 96.6% accurately (Table 4.5). Misclassification by BPNs with one output node is shown in Table 4.6. Patterns from five out of seven dogs (Dogs H, I, S, T, and U) in the evaluation data sets were misclassified using Input Sets 1–8. Most of the misclassification came from LM2 patterns classified as either LM1 or LM3. Most of the LM2 patterns misclassified as LM1 came from six patterns of Dog U, five of which were obtained on the same trial date. All of the LM2 patterns misclassified as LM3 came from particular patterns of three dogs (Dogs S, T, and U). There were several LM3 patterns from two dogs (Dogs H and I) misclassified as LM2. The weakest classification correspondence (i.e, LM1 patterns classified as LM3) came from the same gait attempt of a single dog (Dog U). Note that patterns from only one dog were involved in misclassification using Input Sets 8 and 9.

Misclassification by BPNs with three output nodes is shown in Table 4.7. Patterns from five out of seven dogs (Dogs G, H, I, T, and U) in the evaluation data sets were misclassified using Input Sets 1–8. Most of the misclassification came from LM2 patterns classified as either LM1 or LM3. All of the LM2 patterns misclassified as LM1 came from six patterns of Dog U, five of which were obtained on the same trial date. All of the LM2 patterns

misclassified as LM3 came from particular patterns of two dogs (Dogs U and T). There were several LM3 patterns from three dogs (Dogs G, H, and I) misclassified as LM2. The weakest classification correspondence (i.e, LM1 patterns classified as LM3) came from the same gait attempt of a single dog (Dog U). Note that patterns from only one dog were involved in misclassification using Input Sets 4–9.

Misclassification by PNNs is shown in Table 4.8. Patterns from five out of seven dogs (Dogs H, I, S, T, and U) in the evaluation data sets were misclassified using the Input Sets 1–8. Most of the misclassification came from LM2 patterns classified as either LM1 or LM3. All of the LM2 patterns misclassified as LM1 came from six patterns of Dog U, five of which were obtained on the same trial date. All of the LM2 patterns misclassified as LM3 came from particular patterns of three dogs (Dogs S, T, and U). There were several LM3 patterns from two dogs (Dogs H and I) misclassified as LM2. The weakest classification correspondence (i.e, LM3 patterns classified as LM1) came from particular patterns of two dogs (Dogs H and I) when Input Sets 8–9 were used. In addition, the weakest classification correspondence (i.e, LM1 patterns classified as LM3) came from the same gait attempt of a single dog (Dog U). Note that two to four dogs were involved in misclassification using each input set.

The performance of all the models using Data Configuration 2 was slightly better than their performance using Data Configuration 1. Using the nine sets of input variables with Data Configuration 2, the ANNs differentiated three classes of lameness 97.5% to 100% accurately (Table 4.5). BPNs differentiated three classes 100% accurately using several different sets of input variables. PNNs did not perform as well as BPNs; however, they still classified 97.5–99.6% accurately.

Misclassification by BPNs with one output node is shown in Table 4.9. Using Input Sets 4 and 5, the networks differentiated three classes of lameness 100% accurately. Using the rest of the input sets, patterns from three out of seven dogs (Dogs A, B, and L) in the evaluation data sets were misclassified. LM2 patterns misclassified as LM3 came from particular patterns of two dogs (Dogs B and L), and LM3 patterns misclassified as LM2 were

from patterns from a particular trial date of a single dog (Dog A). No more than one dog was misclassified except when Input Set 2 was used. These BPNs differentiated normal and abnormal gait 100% accurately because normal patterns (LM1) were never misclassified as abnormal (LM2 or LM3) and abnormal patterns (LM2 or LM3) were never misclassified as normal (LM1).

Misclassification by BPNs with three output nodes is shown in Table 4.10. Using Input Sets 4–8, the networks differentiated three classes of lameness 100% accurately. Using the rest of the input sets, patterns from three out of seven dogs (Dog A, B, and L) in the evaluation data sets were misclassified. LM2 patterns misclassified as LM3 came from particular patterns of two dogs (Dogs B and L), and LM3 patterns misclassified as LM2 were from patterns from a particular trial date of a single dog (Dog A). No more than one dog was misclassified except when Input Set 2 was used. These BPNs differentiated normal and abnormal gait 100% accurately because normal patterns (LM1) were never misclassified as abnormal (LM2 or LM3) and abnormal patterns (LM2 or LM3) were never misclassified as normal (LM1).

Misclassification by PNNs with three output nodes is shown in Table 4.11. Using any of the Input Sets, the networks did not differentiate three classes of lameness 100% accurately. Patterns from three out of seven dogs (Dogs A, B, and L) in the evaluation data sets were misclassified. LM2 patterns misclassified as LM3 came from particular patterns of two dogs (Dogs B and L), and LM3 patterns misclassified as LM2 were from patterns from a particular trial date of a single dog (Dog A). Two dogs (Dogs A and L) were misclassified except when Input Set 1 was used. These PNNs differentiated normal and abnormal gait 100% accurately because normal patterns (LM1) were never misclassified as abnormal (LM2 or LM3) and abnormal patterns (LM2 or LM3) were never misclassified as normal (LM1).

Comparing the three ANN models used indicates that BPNs with three output nodes are preferable because BPNs with three output nodes consistently performed as well as or better than BPNs with one output node and PNNs (Table 4.5). The exception was when input variable sets 8 and 9 were presented to the network using Data Configuration 1. How-

ever, the difference between BPNs with one output node and three output nodes was very small. The highest accuracy that each model reached was the same using both data configurations (Table 4.5). In addition, since most of the misclassification came from patterns from a particular trial date for particular dogs regardless of the ANN model used, the classification tendency of all three models was almost the same (Tables 4.6–4.11).

#### 4.2.2 PREFERRED SET OF INPUT VARIABLES

Except for PNNs developed using Data Configuration 2, better results were obtained using both Mid(R-L)/FRONT and Mid(R-L)/HIND instead of using Mid(R-L)/FRONT alone (Table 4.5). Comparing the nine sets of input variables used by BPNs with three output nodes indicates that the combination of Mid(R-L)/FRONT, Mid(R-L)/HIND, and PFz(RH) (Input Set 5) generalized well across different data configurations (Table 4.5 and Figure 4.1). PNNs also performed best using Input Set 5 (Table 4.5 and Figure 4.2). BPNs with one output node approximated the target values more closely using Input Set 8 (Table 4.5 and Figure 4.3). However, using Input Set 8, BPNs with three output nodes, which were found to be the most suitable ANN architecture in this study, did not perform as well as when using Input Set 5 (Table 4.5). Input variables that affect the magnitude of Mid Point were also found to be useful in several cases. These variables included the peak vertical forces of individual limbs, the average falling slope of RF, the average rising slope of RH, and the temporal components of vertical forces.

#### 4.3 SELECTION OF PREFERRED NUMBER OF BPN HIDDEN NODES

Limited analysis of the preferred number of hidden nodes for BPNs was conducted using Mid(R-L)/FRONT, Mid(R-L)/HIND, and PFz(RH). Comparing the preferred number of hidden nodes for BPNs with one output node indicates that two hidden nodes are suitable for this model (Figure 4.4). Comparing the preferred number of hidden nodes for BPNs with

three output nodes indicates that with two or more hidden nodes, the networks accuracy increased (Figure 4.5). With one input node, all the LM3 patterns were misclassified as LM2.

#### 4.4 PREFERRED ANN MODEL AND SET OF INPUT VARIABLES

Given the results presented above, BPNs with three output nodes and two hidden nodes were found to be the most suitable ANN model. In addition, Mid(R-L)/FRONT, Mid(R-L)/HIND, and PFz(RH) comprised the preferred set of input variables.

Table 4.1: Overall Accuracy (%) Using a Conventional Single Input Variable, Data Configuration 1, Evaluation Data Set

Input	Limbs					
	RF	RH	LF	LH	RF-LF	RH-LH
<b>PFz</b>	50.5	48.5	52.5	57.8	48.0	64.7
<b>IFz</b>	39.2	51.5	48.5	58.3	-	-
<b>TFz</b>	54.1	47.1	48.5	54.9	-	-
<b>AveR</b>	50.5	47.1	48.5	57.4	-	-
<b>AveF</b>	57.4	51.0	45.1	57.8	-	-
<b>TotalT</b>	39.7	48.0	49.0	48.5	-	-
<b>PFy-b</b>	48.5	42.2	48.5	52.5	-	-
<b>IFy-b</b>	48.5	48.5	48.5	53.9	-	-
<b>PFy-p</b>	45.1	41.2	48.5	59.8	-	-
<b>IFy-p</b>	45.6	47.6	48.5	56.9	-	-
<b>PFx</b>	42.7	46.6	46.6	48.5	-	-
<b>TotalT-TFz</b>	61.8	-	46.1	-	-	-
<b>WB</b>	-	-	-	61.3	-	-

Table 4.2: Overall Accuracy (%) Using a Single Input Variable Suggested in This Study, Data Configuration 1, Evaluation Data Set

Normalized by Peak Vertical Force of	Mid(R)	Mid(R-L)
—	56.9	55.4
<b>FRONT</b>	56.9	<b>93.6</b>
<b>HIND</b>	57.4	<b>90.7</b>
<b>RF+LH</b>	57.4	55.9
<b>LF+RH</b>	57.4	55.4
<b>RIGHT</b>	56.9	63.2
<b>LEFT</b>	57.8	<b>90.7</b>
<b>RF+LF+LR</b>	56.4	56.4
<b>RR+LF+LR</b>	55.9	56.9
<b>RF+RR+LR</b>	55.9	56.4
<b>RF+RR+LF</b>	55.4	56.9
<b>ALL</b>	56.4	63.7

Table 4.3: Overall Accuracy (%) Using Combinations of the Three Best Single Input Variables, Data Configuration 1, Evaluation Data Set

Input			OA
Mid(R-L) /FRONT	Mid(R-L) /HIND	Mid(R-L) /LEFT	
*	*	*	93.6 90.7 90.7
* *	* *	* *	<b>95.6</b> 94.1 88.7
*	*	*	92.7

\* Input variables mapped by ANNs

Table 4.4: Overall Accuracy (%) Using Mid(R-L)/FRONT, Mid(R-L)/HIND and Other Variables, Data Configuration 1, Evaluation Data Set

Mid(R-L)		PFz				AveF	AveR	TotalT-TFz	TFz	OA
/FRONT	/HIND	(RF)	(RH)	(LF)	(LH)	(RF)	(RH)	(RF)	(RR)	
*	*									95.6
*	*	*								95.1
*	*		*							92.7
*	*			*						96.1
*	*				*					87.8
*	*					*				94.6
*	*						*			95.6
*	*							*		94.6
*	*								*	95.6
*	*	*	*							95.1
*	*					*	*			94.6
*	*							*	*	92.7
*	*	*				*	*			94.6
*	*		*			*	*			94.6
*	*	*	*			*				95.6
*	*	*	*				*			95.6
*	*	*	*			*	*			96.6
*	*	*	*			*	*	*		96.1
*	*	*	*			*	*		*	96.1
*	*	*	*			*	*	*	*	96.1

\* Input variables mapped by ANNs

Table 4.5: Overall Accuracy (%) Using Mid(R-L)/FRONT, Mid(R-L)/HIND and Other Variables, Data Configurations 1 and 2, Evaluation Data Sets

Input Set	Mid(R-L)/FRONT	Mid(R-L)/HIND	PFz (RF)	PFz (RH)	PFz (LF)	PFz (LH)	AveF (RF)	AveR (RH)	TotalT-TFz (RF)	TFz (RR)
1	*									
2		*								
3	*	*								
4	*	*	*							
5	*	*		*						
6	*	*			*					
7	*	*				*				
8	*	*	*	*			*	*		
9	*	*	*	*			*	*	*	*

Input Set	Data Configuration 1			Data Configuration 2		
	BPN 1	BPN 3	PNN 3	BPN 1	BPN 3	PNN 3
1	93.6	95.6	93.6	99.6	99.6	99.6
2	90.7	94.1	93.1	97.5	97.5	97.5
3	95.6	95.6	95.6	99.6	99.6	98.3
4	95.1	95.6	94.6	100	100	98.7
5	92.7	96.6	96.1	100	100	98.7
6	96.1	96.1	96.1	99.6	100	98.3
7	87.8	96.6	94.1	99.6	100	98.3
8	96.6	95.6	94.6	99.6	100	98.3
9	96.1	94.6	95.1	99.6	100	98.3

\* Input variables mapped by ANNs

Table 4.6: Misclassification by BPN with One Output Node, Data Configuration 1, Evaluation Data Set

Dog	U			I			H		S	T		
Trial Date	T <sub>-1</sub>	T <sub>1</sub>	T <sub>9</sub>	T <sub>3</sub>	T <sub>6</sub>	T <sub>9</sub>	T <sub>12</sub>	T <sub>1</sub>	T <sub>1</sub>	T <sub>1</sub>	T <sub>3</sub>	
Actual Score	LM1	LM2	LM2	LM2	LM2	LM3	LM2	LM3	LM2	LM2	LM2	
Input Set	Misclassified as (Number of patterns)											
1	LM3(1)*	LM1(1)	LM3(3)	LM1(5)						LM3(3)		
2	LM2(1)	LM1(1)		LM1(5)	LM1(1)	LM1(5)	LM2(1)		LM2(1)		LM3(3)	LM3(1)
3	LM2(1)	LM1(1)		LM1(5)			LM2(1)		LM2(1)			
4	LM3(1)	LM1(1)	LM3(2)	LM1(5)							LM3(1)	
5	LM3(1)	LM1(1)	LM3(3)	LM1(5)						LM3(3)	LM3(2)	
6	LM2(1)	LM1(1)		LM1(5)			LM2(1)					
7	LM2(1)	LM1(1)	LM3(4)	LM1(5)		LM1(2)	LM2(1)	LM1(2)		LM3(4)	LM3(3)	LM3(2)
8	LM2(1)	LM1(1)		LM1(5)								
9	LM3(1)	LM1(1)	LM3(1)	LM1(5)								

\* Dog U LM1 pattern acquired on T<sub>-1</sub> misclassified as LM3

Table 4.7: Misclassification by BPN with Three Output Nodes, Data Configuration 1, Evaluation Data Set

Dog	U				T	H	I	G
Trial Date	T <sub>-1</sub>	T <sub>1</sub>	T <sub>9</sub>	T <sub>1</sub>	T <sub>1</sub>	T <sub>9</sub>	T <sub>6</sub>	
Actual Score	LM1	LM2	LM2	LM2	LM3	LM3	LM3	
Input Set	Misclassified as (Number of patterns)							
1	LM2(1)*	LM1(1)		LM1(5)			LM2(1)	LM2(1)
2	LM2(1)	LM1(1)		LM1(5)	LM3(1)	LM2(2)	LM2(2)	
3	LM2(1)	LM1(1)		LM1(5)		LM2(1)	LM2(1)	
4	LM3(1)	LM1(1)	LM3(2)	LM1(5)				
5	LM2(1)	LM1(1)		LM1(5)				
6	LM3(1)	LM1(1)	LM3(1)	LM1(5)				
7	LM3(1)			LM1(5)	LM3(1)			
8	LM3(1)	LM1(1)	LM3(2)	LM1(5)				
9	LM3(1)	LM1(1)	LM3(4)	LM1(5)				

\* Dog U LM1 pattern acquired on T<sub>-1</sub> misclassified as LM2

Table 4.8: Misclassification by PNN, Data Configuration 1, Evaluation Data Set

Dog	U				S	T	H	I
Trial Date	$T_{-1}$	$T_1$	$T_9$	$T_1$	$T_1$	$T_1$	$T_1$	$T_9$
Actual Score	LM1	LM2	LM2	LM2	LM2	LM2	LM3	LM3
Input Set	Misclassified into (Number of patterns)							
1	LM3(1)*	LM1(1)	LM3(3)	LM1(5)	LM3(3)	LM3(3)	LM2(2)	LM2(2)
2	LM2(1)	LM1(1)		LM1(5)				
3	LM2(1)	LM1(1)		LM1(5)				
4	LM2(1)	LM1(1)		LM1(5)				
5	LM2(1)	LM1(1)		LM1(5)				
6	LM2(1)	LM1(1)	LM1(5)	LM3(2)	LM2(1)	LM2(1)		
7	LM2(1)	LM3(1)	LM1(5)					
8	LM3(1)		LM1(2)				LM3(1)	LM1(5)
9	LM3(1)	LM1(1)	LM3(1)				LM1(5)	

\* Dog U LM1 pattern acquired on  $T_{-1}$  misclassified as LM3

Table 4.9: Misclassification by BPN with One Output Node, Data Configuration 2, Evaluation Data Set

Dog	A	B	L
Trial Date	$T_{12}$	$T_3$	$T_1$
Actual Score	LM3	LM2	LM2
Input Set	Misclassified as (Number of patterns)		
1	LM2(5)*	LM3(1)	
2			LM3(1)
3			LM3(1)
4			
5			
6		LM3(1)	
7			LM3(1)
8			LM3(1)
9			LM3(1)

\* Dog A LM3 pattern acquired on  
 $T_{12}$  misclassified as LM2

Table 4.10: Misclassification by BPN with Three Output Nodes, Data Configuration 2, Evaluation Data Set

Dog	A	B	L
Trial Date	T <sub>12</sub>	T <sub>3</sub>	T <sub>1</sub>
Actual Score	LM3	LM2	LM2
Input Set	Misclassified as (Number of patterns)		
1	LM2(5)*	LM3(1)	LM3(1) LM3(1)
2			
3			
4			
5			
6			
7			
8			
9			

\* Dog A LM3 pattern acquired on  
T<sub>12</sub> misclassified as LM2

Table 4.11: Misclassification by PNN, Data Configuration 2, Evaluation Data Set

Dog	A	B	L
Trial Date	$T_{12}$	$T_3$	$T_1$
Actual Score	LM3	LM2	LM2
Input Set	Misclassified as (Number of patterns)		
1		LM3(1)	
2	LM2(5)*		LM3(1)
3	LM2(3)		LM3(1)
4	LM2(2)		LM3(1)
5	LM2(3)		LM3(1)
6	LM2(3)		LM3(1)
7	LM2(2)		LM3(2)
8	LM2(2)		LM3(2)
9	LM2(2)		LM3(2)

\* Dog A LM3 pattern acquired on  
 $T_{12}$  misclassified as LM2

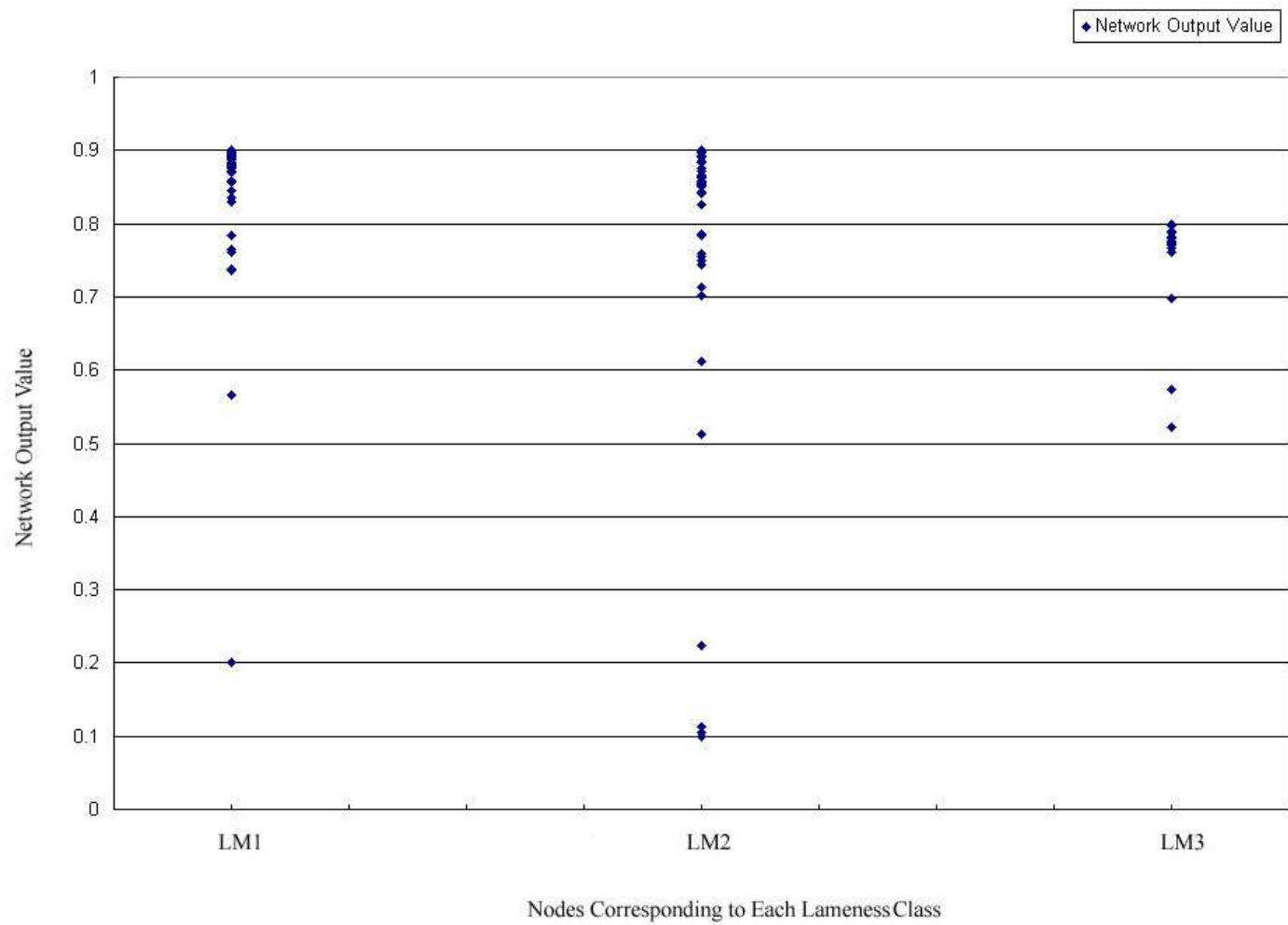


Figure 4.1: BPN with Three Output Nodes Using Mid(R-L)/FRONT, Mid(R-L)/HIND, and PFz(RH) (Data Configuration 1)

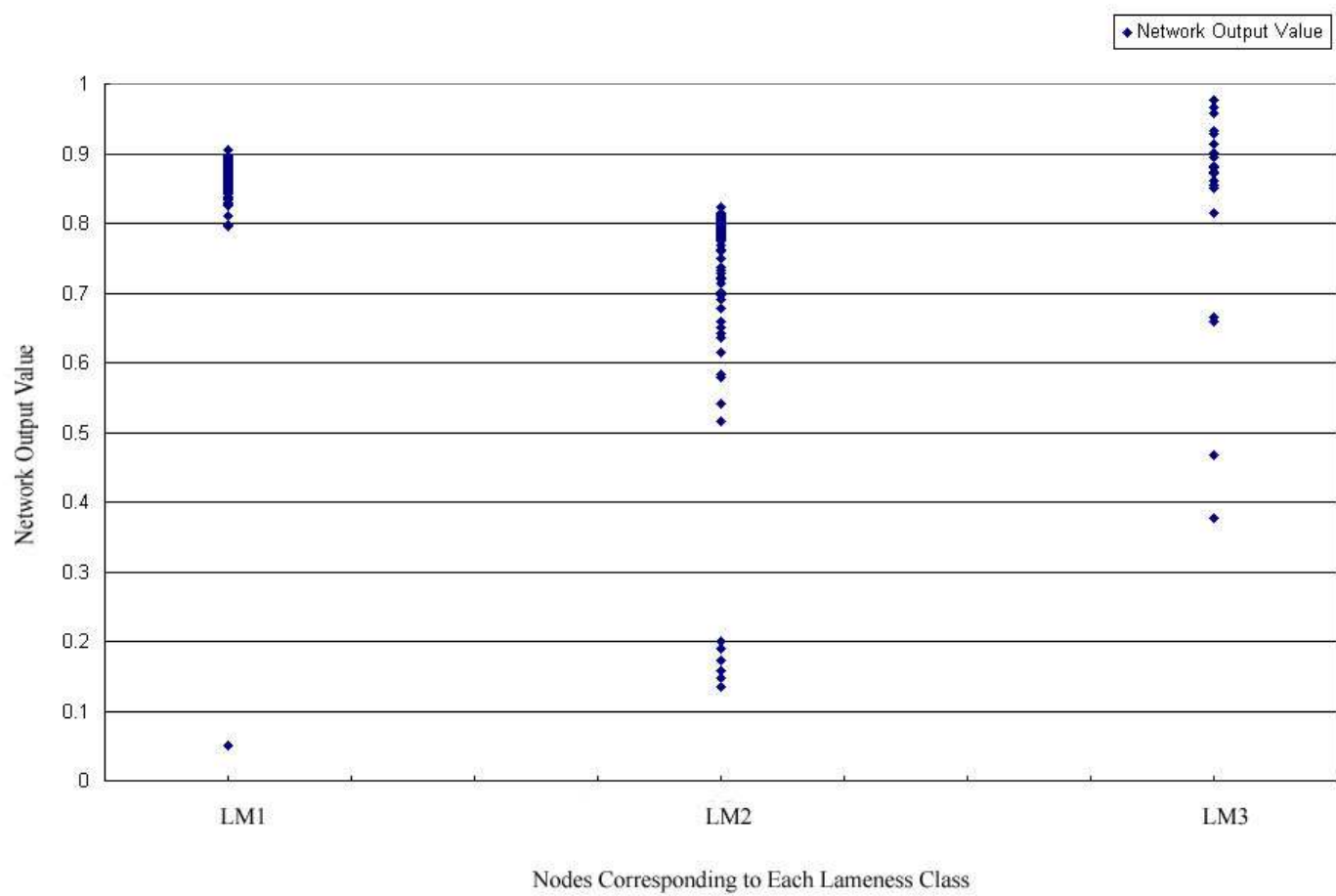


Figure 4.2: PNN Using Mid(R-L)/FRONT, Mid(R-L)/HIND, and PFz(RH) (Data Configuration 1)

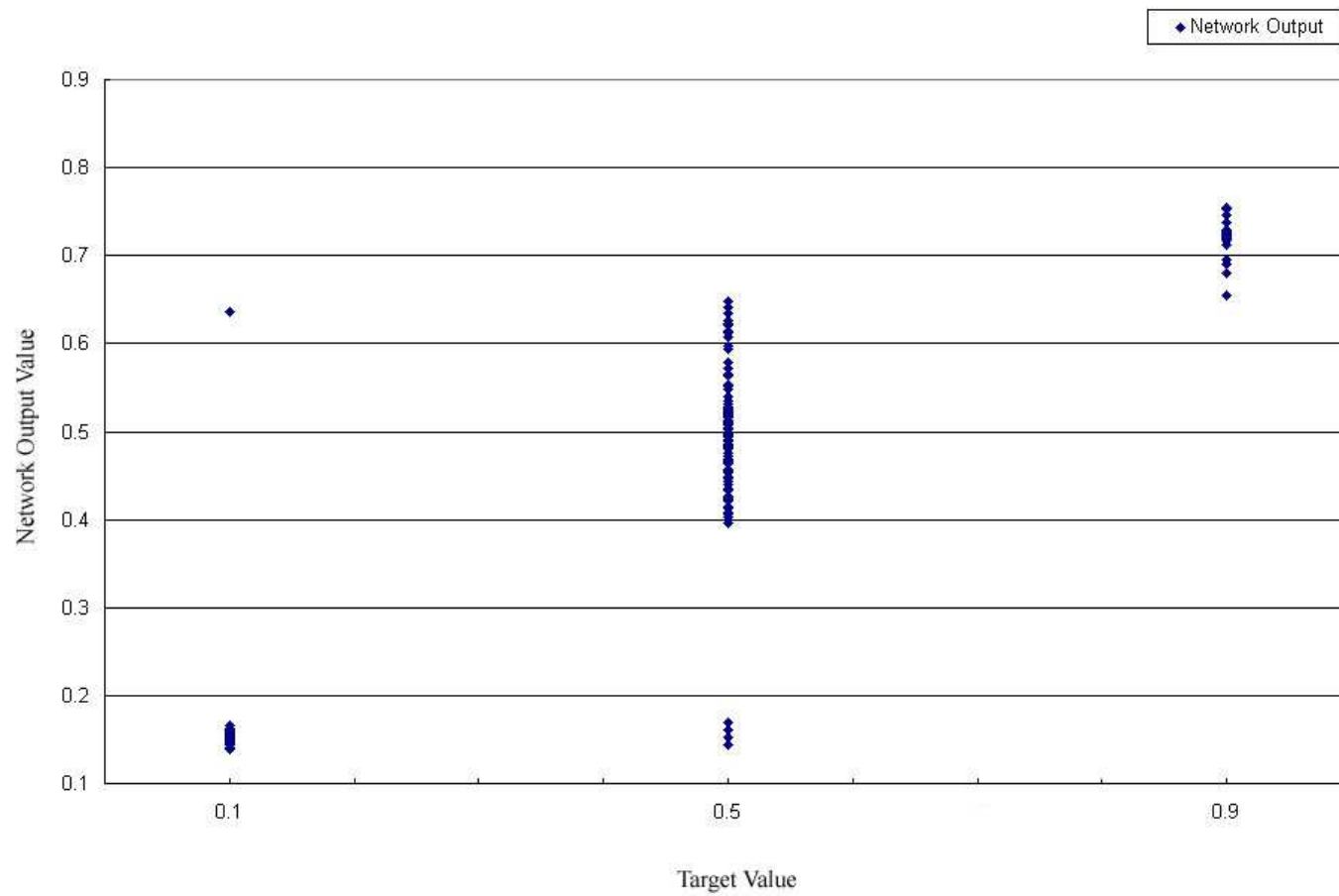


Figure 4.3: BPN with One Output Node Using Mid(R-L)/FRONT, Mid(R-L)/HIND, PFz(RF), PFz(RH), AveF(RF), and AveR(RH) (Data Configuration 1)

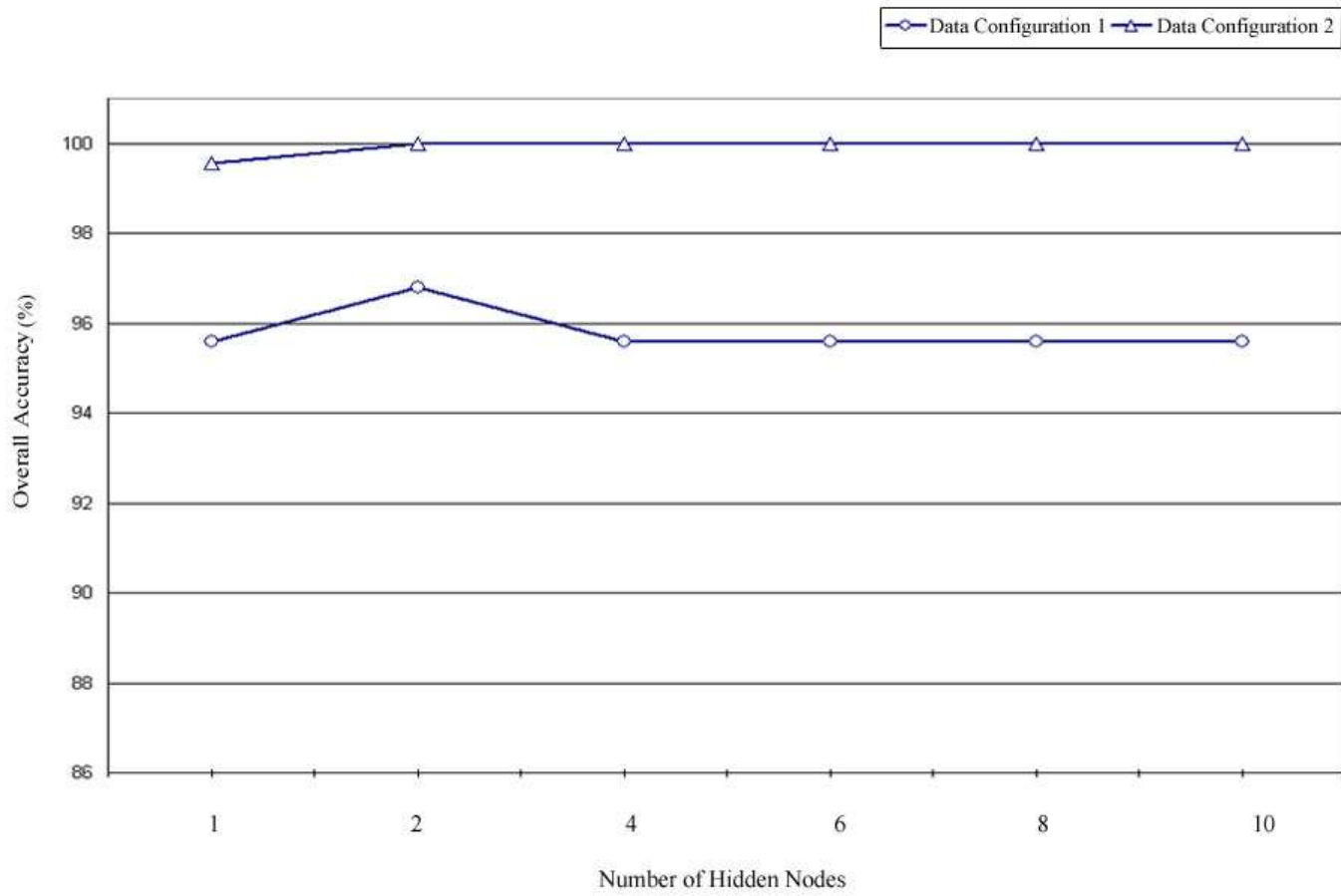


Figure 4.4: Hidden Node Analysis (BPN with One Output Node)

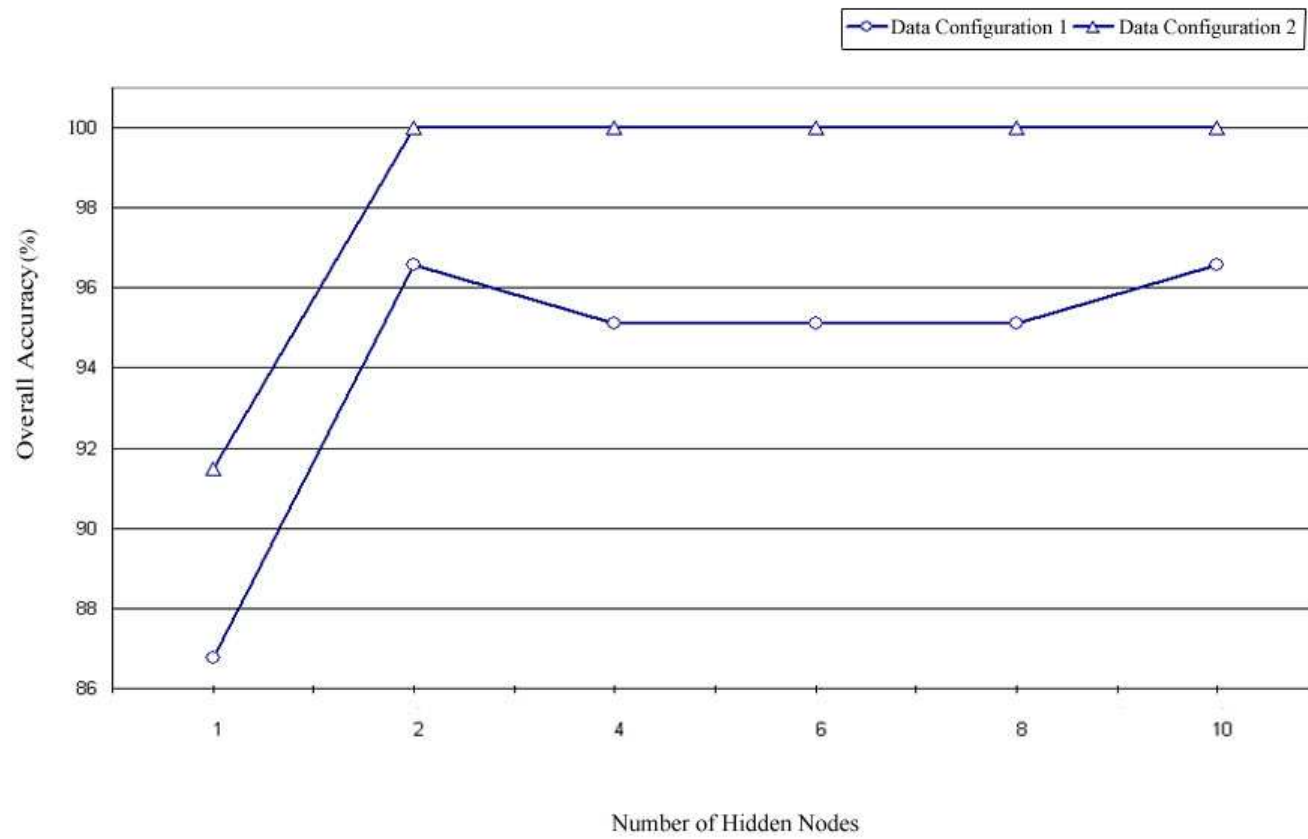


Figure 4.5: Hidden Node Analysis (BPN with Three Output Nodes)

## CHAPTER 5

### SUMMARY AND CONCLUSIONS

#### 5.1 SUMMARY

ANNs were developed to map GRF variables to duplicate subjective diagnostic scores of lameness. The data were gathered from clinically normal dogs that underwent left hind limb cranial cruciate ligament transection, inducing osteoarthritis in the stifle joint. This study focused on identifying single input variables that significantly influenced ANN performance and finding the preferred ANN model and set of input variables. The three ANN models considered were (a) BPN with one output node, (b) BPN with three output nodes, and (c) PNN with three output nodes. The accuracy of the ANNs and input variables was tested on two different data configurations, each of which never contained patterns from the same dog in both model development and evaluation.

The three single input variables found to be useful in this study included the difference between Mid Points of the non-injured and injured sides of the dog normalized by the sum of the peak vertical forces of (a) the two front, (b) the two hind, or (c) the two left limbs. BPNs with three output nodes were found to be the most accurate ANN models. The preferred set of input variables for this model included the difference between Mid Points of the non-injured and injured sides of the dog normalized by the sum of the peak vertical forces of (a) the two front limbs and (b) the two hind limbs and the peak vertical force of the contralateral limb (RH). Using the preferred set of input variables found in this study, BPNs with three output nodes differentiated three classes of lameness with 96.6–100% accuracy. Including the peak vertical forces of other individual limbs, average falling slope of the diagonal limb (RF),

average rising slope of the contralateral limb (RH), and temporal variables associated with vertical forces slightly increased the overall accuracy.

## 5.2 CONCLUSIONS

The results of this study suggest that ANNs provide a way to use canine GRF data to predict subjective lameness scores. The results corroborate the findings of similar human and equine gait studies discussed in Chapter 1. The results are promising, considering the small number of patterns and dogs used for model development, the uneven number of training patterns from each class, and the subjective target values. ANNs have been shown to generalize well if there are more patterns for model development. In addition, it is ideal to have the same number of patterns for each class for model development so that examples from each class have nearly the same influence on the network (Smith, 1993). The results confirm that ANNs work well with limited canine GRF data if appropriate input variables are used.

### 5.2.1 SIGNIFICANCE

The results of this study indicate that computerized analysis of GRF data using ANNs allows for more accurate diagnosis by detecting signs of lameness that could be missed by GRF data analysis done by a clinician. GRF curves obtained from Dog A before the surgery (assigned LM1 by a veterinarian) and GRF curves obtained from the same dog after the surgery (assigned LM3 by a veterinarian) are superimposed for comparison in Figure 5.1. The shape of the post-operative GRF curves are quite similar to those obtained before the surgery. In addition, the peak vertical force of injured limb (LH) was higher than the preoperative value. Furthermore, the peak vertical force of injured limb (LH) was higher than the contralateral limb (RH) after the surgery. These findings contradict the findings of other studies (DeCamp, 1997; Jevens et al. 1996; Rumph et al., 1995). As a result, there is a great possibility that lameness revealed in the gait data could be missed by a clinician. However, ANNs developed in this study successfully classified the post-operative pattern as LM3 using

appropriate input variables. This finding demonstrates the benefit of computerized analysis of GRF data: adding accuracy and consistency to clinical decision making.

Furthermore, the results of this study indicate that canine gait analysis and diagnosis systems using ANNs could be both time efficient and cost effective. As Simon (2004) discussed, the clinical use of human gait analysis and diagnosis systems is most limited by the time and cost required for gait testing and interpretation. Canine GRF data can be readily obtained simply by trotting the dog on a force-plate. In addition, the results of this study indicate that only a few gait attempts are required to obtain a fairly accurate diagnosis and that ANNs can instantaneously interpret data if successfully interfaced with data acquisition software. Hence, canine gait analysis and diagnosis systems using ANNs could be financially reimbursable. As a result, canine gait analysis and diagnosis systems using ANNs are expected to be used extensively and have a significant clinical impact. The gait data used in this study were obtained from dogs with artificially induced osteoarthritis for new drug development research. Osteoarthritis is one of the most common causes of chronic pain in dogs; around 20% of the canine population (10 to 12 million dogs in the United States alone) is affected (Budsberg, 2004). Hence, computerized gait analysis systems that add accuracy, consistency, and efficiency to pharmacological research could benefit a large percentage of the canine population. In addition, these systems can be used in clinical decision support to provide more appropriate treatment or provide more precise evaluation of surgical and pharmacological intervention.

### 5.2.2 LIMITATIONS OF THE STUDY AND POSSIBLE FUTURE IMPROVEMENT

The limiting assumptions of this study are provided below with a view to future improvement. First, BPNs were trained only once with random initial weights. Because BPNs learn in order to minimize error from a particular place of the search space, they might find local optima and leave global optima undiscovered. Hence, initial weights could be re-randomized and BPNs could be re-trained to see if a global minimum error could be found.

Second, vertical impulses of injured limbs were presented to the network; however, they did not produce good results. If the Mid Point was higher than 33% of the peak vertical force of the ipsilateral front limb, the impulses were attributed to the front limbs. In actuality, some of the impulses should have been attributed to the hind limbs. Since the vertical impulses of injured limbs were found to be useful in many previous studies (Budsberg, 2001; Budsberg et al., 1988; DeCamp, 1997; Jevens et al., 1996; O'Connor et al., 1989; Rumph et al., 1995), the method introduced by Lee et al. (2002) could be used to reconstruct the vertical impulses of individual limbs.

Third, accuracy of each ANN model was analyzed individually. However, since all three ANN models performed well, future researchers could develop ensembles that train individual networks using the same data set and optimize by combining the results from each network. In addition, ANNs with different architecture parameters such as initial weights, learning rate, momentum, number of hidden nodes, and input variables could be trained in parallel to obtain the final results. A detailed explanation of ensemble networks and their potential can be found in Engelbrecht (2002).

Fourth, the input analysis was done by heuristic search using knowledge from previous studies and biomechanical analysis of the canine gait. This process was time-consuming and may have left other optimal combinations undiscovered. Hence, some other computational means, such as genetic algorithms, could be tried to see whether there are other combinations of variables that would work as well as or better than the combinations considered in this study. In addition, while an individual input variable is interpretable, understanding why one combination of input variables works better than another is difficult. More detailed biomechanical analysis has to be done to obtain conclusive interpretation of the variables.

Fifth, ANNs only differentiated three broadly-defined classes of lameness. However, in real practice, it would be useful to have a confidence factor or probability for each classification, as in other Expert Systems in biomedicine. In addition, it would also be useful to find more precise values, instead of only LM1, LM2, and LM3. One way to obtain these values is to

convert the closeness of target value approximation. The other possible approach is to create a neuro-fuzzy system. The major advantage of using a fuzzy system is that it quantifies the degree to which gait data belongs to a certain lameness class. Fuzzy clustering methods have been applied to gait data, and neuro-fuzzy systems have been developed for other classification problems in biomedicine (Chau, 2001[a]; Hudson & Cohen, 2000; Lisboa, 2002; O'Malley et al., 1997; Tan et al., 1999 and Teodorescu, 1999). O'Malley et al. (1997) applied a fuzzy clustering technique to gait data collected from children with cerebral palsy in order to measure gait changes after neuro-surgical and orthopedic operations. Tan et al. (1999) also used a fuzzy clustering technique to differentiate the gait of Parkinson's disease patients from the gait of neurologically intact subjects.

Sixth, patterns that showed no weightbearing in the injured limb were not used. Hence, accuracy of ANN models and input variables found to be preferable in this study have to be further investigated with data sets that contain more patterns that show no weightbearing in the injured limb. However, in a hybrid ANN Expert System, these patterns could be classified as LM4 according to a simple rule: IF no weightbearing, THEN LM4. However if this rule were used, precise values could not be obtained for gaits with lameness severity between LM3 and LM4. Hence, whether an ANN or another means is used to classify the non-weightbearing patterns should be determined according to how the system will be applied.

Seventh, as Chau (2001 [b]) discussed, ANN-based research has more often been used for human gait analysis than other methods. Chau attributed the infrequent use of gait analysis systems in clinical practice to the black-box quality of ANNs, in spite of their accuracy. Hence, it is necessary to find a way to incorporate Expert Systems that can provide explanations to support the conclusions of ANNs.

Eighth, only similar-built dogs with osteoarthritis induced by CCLT were used. Previous studies reported that peak vertical forces and impulses correlated with physical size of the dog (DeCamp, 1997). Hence, it would be interesting to compare these results with the results from various kinds and sizes of dogs with natural osteoarthritis.

Finally, the subjective diagnostic score was provided by only one veterinarian. It would be interesting see whether the preferred ANN model and set of input variables found in this study would also be effective in mapping GRF data to subjective diagnostic scores given by other veterinarians.

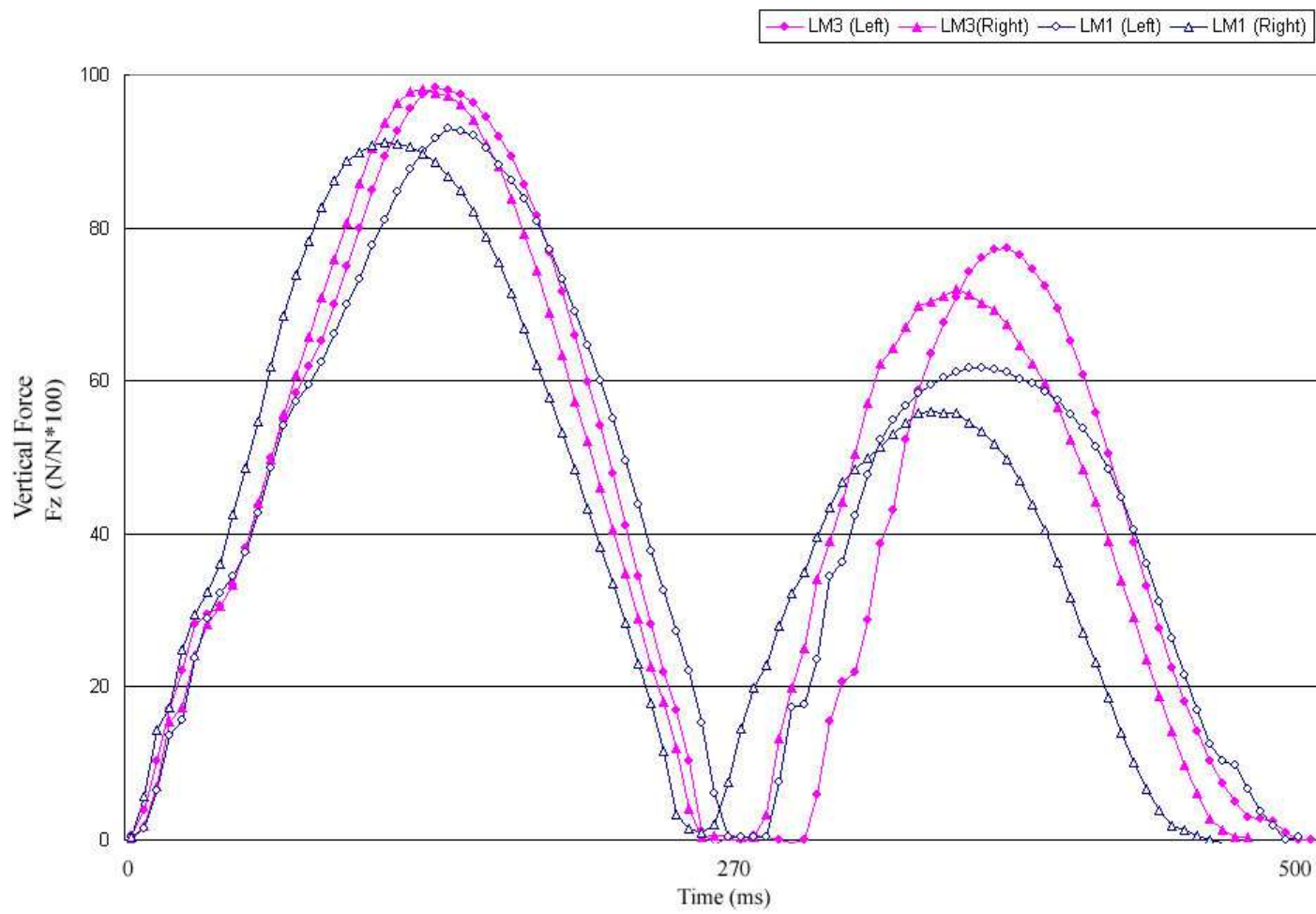


Figure 5.1: LM1 and LM3 Vertical GRF Curves Acquired from Dog A

## REFERENCES

- Begg, R., and Kamruzzaman, J. (2005) A machine learning approach for automated recognition of movement patterns using basic, kinetic and kinematic gait data. *Journal of Biomechanics* 38.3: 401–408.
- Berton, J.G., and Lee, A. (1997) An application of neural networks for distinguishing gait patterns on the basis of hip-knee joint angle diagrams. *Gait & Posture* 5: 28–33.
- Brown, Curtis M. (1986) *Dog locomotion and gait analysis*. Wheat Ridge, CO: Hoffin Publishing.
- Budsberg, Steven C. (2001) Long-term temporal evaluation of ground reaction forces during development of experimentally induced osteoarthritis in dogs. *American Journal of Veterinary Research* 62.8: 1207–1211.
- Budsberg, Steven C. (2004) Managing the pain caused by osteoarthritis. *Ettinger's Insights in Internal Medicine* 2:1 1–5.
- Budsberg, Steven C.; Verstraete, Mary C.; and Soutas-Little, Robert W. (1987) Force plate analysis of the walking gait in healthy dogs. *American Journal of Veterinary Research* 48.6: 915–918.
- Budsberg, Steven C.; Verstraete, Mary C.; Soutas-Little, Robert W.; Flo, G. L.; and Probst, C. W. (1988) Force plate analyses before and after stabilization of canine stifles for cruciate injury. *American Journal of Veterinary Research* 49.9: 1522–1524.
- Budsberg, Steven C.; Jevens, Dermot J.; Brown, John; Foutz, Tim L.; DeCamp, Charles E.; and Reece, Lynn (1993) Evaluation of limb symmetry indices, using ground reaction forces in healthy dogs. *American Journal of Veterinary Research* 54.10: 1569–1574.

- Budsberg, Steven C.; Verstraete, Mary C.; Brown, John; and Reece, Lynn (1993) Vertical loading rates in clinically normal dogs at trot. *American Journal of Veterinary Research* 56.10: 1275–1280.
- Budsberg, Steven C.; Chambers, Jonathan N.; VanLue, Stephen L.; Foutz, Tim L.; and Reece, Lynn (1996) Prospective evaluation of ground reaction forces in dogs undergoing unilateral total hip replacement. *American Journal of Veterinary Research* 57.12: 1781–1785.
- Budsberg, Steven C.; Johnston, Spencer A.; Schwarz, P. D.; DeCamp, Charles E.; and Claxton, R. (1999) Efficacy of etodolac for the treatment of osteoarthritis of the hip joint in dogs. *Journal of the American Veterinary Medical Association* 214.2: 206–210.
- Chau, Tom (2001 [a]) A review of analytical techniques for gait data. Part 1: Fuzzy, statistical and fractal methods. *Gait and Posture* 13: 49–66.
- Chau, Tom (2001 [b]) A review of analytical techniques for gait data. Part 2: Neural network and wavelet methods. *Gait and Posture* 13: 102–120.
- Cheron, G.; Leurs, F.; Bengoetxea, A.; Draye, J.P.; Destrée M.; and Dan, B. (2003) A dynamic recurrent neural network for multiple muscle electromyographic mapping to elevation angle of the lower limb in human locomotion. *Journal of Neuroscience Methods* 129: 95–104.
- Cross, Alan R.; Budsberg, Steven C.; and Keefe, Thomas J. (1997) Kinetic gait analysis assessment of meloxicam efficacy in a sodium urate-induced synovitis model in dogs. *American Journal of Veterinary Research* 58.6: 626–631.
- DeCamp, Charles E. (1997) Kinetic and kinematic gait analysis and the assessment of lameness in the dog. *Veterinary Clinics of North America: Small Animal Practice* 27.4: 825–840.

- Dueland, R.; Bartel, D. L.; and Antonson, E. (1977) Force plate technique for canine gait analysis of total hip and excision arthroplasty. *Journal of the American Animal Hospital Association* 13.5: 547–552.
- Engelbrecht, Andries P. (2002) *Computational intelligence: An introduction*. Chichester, England: John Wiley & Sons.
- Evans, R.; Horstman, C.; and Conzenmius, M. (2003) Force platform gait analysis as a diagnostic test. *Veterinary Orthopedic Society Annual Conference*
- Gray, James (1968) *Animal locomotion*. New York: W. W. Norton & Company.
- Hahn, Michael E.; Farley, Arthur M.; Lin, Victor; and Chou, Li-Shan (2005) Neural network estimation of balance control during locomotion. *Journal of Biomechanics* 38.4: 717–724.
- Hollenbeck, Leon (1981) *The dynamics of canine gait: A study of motion* Fairfax, VA: Denlinger's Publishers.
- Huang C.J. (2004) Class prediction of cancer using probabilistic neural networks and relative correlation metric. *Applied Artificial Intelligence* 18.2: 117-128.
- Huang, C.J. and Liao, W.C. (2004) Application of probabilistic neural networks to the class prediction of leukemia and embryonal tumor of central nervous system. *Neural Processing Letters* 19.3: 211–226.
- Hudson, Donna L., and Cohen, Maurice E. (2000) *Neural networks and artificial intelligence for biomedical engineering*. New York: The Institute of Electrical and Electronics Engineers.
- Jevens, Dermot J.; DeCamp, Charles E.; Hauptman, Joe; Braden, Terrance D.; Richter, Marlee; and Robinson, Rachel (1996) Use of force-plate analysis of gait to compare two surgical techniques for treatment of cranial cruciate ligament rupture in dogs. *American Journal of Veterinary Research* 57.3: 389–393.

- Keegan, K.G.; Arafat, S.; Skubic, M.; Wilson D.A.; and Kramer, J. (2003) Detection of lameness and determination of the affected forelimb in horses by use of continuous wavelet transformation and neural network classification of kinematic data. *American Journal of Veterinary Research* 64.11: 1376–1381.
- Lafuente, R.; Belda, J.M.; Sánchez-Lacuesta, J.; Soler, C.; and Prat, J. (1997) Design and test of neural networks and statistical classifiers in computer-aded movement analysis: a case study on gait analysis. *Clinical Biomechanics* 13.3: 216–229.
- Leach, Douglas (1993) Recommended terminology of researcher in locomotion and biomechanics of quadrupedal animals. *Acta Anatomica* 146: 130–136.
- Lee, D. V.; Bertram, J. E. A.; Todhunter, R. J.; Williams A. J.; and Lust G. (2002) Force overlap in trotting dogs: A Fourier technique for reconstructing individual limb ground reaction force. *Veterinary and Comparative Orthopaedics and Traumatology* 15.4: 223–227.
- Lisboa, P.J.G. (2002) A review of evidence of health benefit from artificial neural networks in medical intervention. *Neural Networks* 15: 11-39.
- Newton, Charles D., and Nunamaker, David M. (1985) *Textbook of small animal orthopaedics*. Philadelphia: J.B. Lippincott Company.
- McLaughlin, Ron M. (2001) Kinetic and kinematic gait analysis in dogs. *Veterinary Clinics of North America-Small Animal Practice* 31.1: 193–201.
- O'Connor, Brian L.; Vsco, Denise M.; Heck, David A.; Mayers, Stephen L.; and Brandt, Kenneth D. (1989) Gait alternations in dogs after transection of the anterior cruciate ligament. *Arthritis and Rheumatism* 32.9: 1142–1147.
- O'Malley, M.J.; Abel, M.F.; Damiano, D.L.; and Vaughan, C.L. (1997) Fuzzy clustering of children with cerebral palsy based on temporal-distance gait parameters. *IEEE Transactions on Rehabilitation Engineering* 5.4: 300–309.

- Renberg, Walter C.; Johnston, Spencer A.; Ye, Keying; and Budsberg, Steven C. (1999) *American Journal of Veterinary Research* 60.7: 814–819.
- Rumph, P.F.; Kincaid, S.A.; Visco, D.M.; Baird, D.K.; Kammermann, J.R.; and West, M.S. (1995) Redistribution of vertical ground reaction force in dogs with experimentally-induced chronic hindlimb lameness. *Veterinary Surgery* 24.5: 384–389.
- Saini, J.S.; Jain, A.K.; Kumar, S.; Vikal, S.; Pankaj, S.; and Singh, S. (2003) Neural network approach to classify infective keratitis. *Current Eye Research* 27.2: 111-116.
- Schobesberger, H., and Perham, C. (2002) Computerized detection of supporting forelimb lameness in the horse using an artificial neural network. *The Veterinary Journal* 163: 77–84.
- Schöllhorn, W.I. (2004) Applications of artificial neural nets in clinical biomechanics. *Clinical Biomechanics* 19: 876–898.
- Simon, Sheldon R. (2004) Quantification of human motion: Gait analysis—benefits and limitations to its application to clinical problems. *Journal of Biomechanics* 37: 1869–1880.
- Smith, Murray (1993) *Neural networks for statistical modeling* New York: Van Nostrand Reinhold.
- Specht, Donald D. (1990) Probabilistic neural networks. *Neural Networks* 3: 109–118.
- Su, Fong-Chin, and Wu, Wen-Lan (2000) Design and testing of a genetic algorithm neural network in the assessment of gait patterns. *Medical Engineering & Physics* 22: 67–74.
- Tan, T.; Guan, L.; and Burne, J. (1999) A real-time image analysis system for computer-assisted diagnosis of neurological disorders. *Real-time Imaging* 5.4: 253–69.
- Teodorescu, Horia-Nicolai; Kandel, Abraham; and Jain, Lakhmi C. (1999) *Fuzzy and neuro-fuzzy systems in medicine*. New York: CRC Press.

Wu, Wen-Lan; Su, Fong-Chin; Cheng, Yuh-Min; and Chou, You-Li (2001) Potential of the genetic algorithm neural network in the assessment of gait patterns in ankle arthrodesis. *Annals of Biomedical Engineering* 29: 83–91.

Zhao, C.Y.; Zhang, R.S.; Liu, H.X.; Xue, C.X.; Zhao, S.G.; Zhou, X.F.; Liu, M.C.; and Fan, B.T. (2004) Diagnosing anorexia based on partial least squares, back propagation neural network, and support vector machines. *Journal of chemical information and computer sciences* 40.6: 2040–2046.